Quantification of phosphorus release from sediments in Lough Neagh and factors affecting the recovery of water quality

Evidence and Innovation Project, 16/4/02 (48122)

Technical Report

December 2020

James Thompson, Yvonne McElarney

Fisheries and Aquatic Ecosystems Branch, AFBI

Acknowledgements

We would like to thank the funder of this work, the Department for Agriculture, Environment and Rural Affairs in Northern Ireland. We also gratefully acknowledge the support of the Environment Marine and Fisheries Group; Science, Evidence and Innovation Policy Division - Food and Farming Group and Northern Ireland Environment Agency Water Management Unit staff within the Department. We would like to thank Wendy McKinley, Brenda Walker, and Mary Gallagher for their comments on a previous draft of this report.

We would also like to thank Brian Rippey and Julie Campbell of Ulster University for assistance with method development and analysis of results. Furthermore, we would like to thank the following for use of boats and invaluable assistance to retrieve sediment cores from the lakes: Stephen Ryan, Frankie Conlon and Martin Devlin. We also thank AFBI staff, past and present for assistance with field work and water chemistry, especially Kevin Gallagher, Paul Ferguson, Ryan Wightman and Brian Stewart. Thanks for the support from Lough Neagh Fishermen's Co-op. Thanks also to Handong Yang of the Environmental Radiometric Facility at University College London for completing the dating of the sediment cores.

Executive Summary

Lough Neagh has experienced nutrient enrichment over many years and has a large reservoir of stored nutrients in the sediment. Lake sediment generally has considerable capacity to keep these nutrients chemically bound and unavailable to the water column. However, over the last century changes have occurred in the characteristics of the lake leading to a large release of sediment derived phosphorus (P) during the summer. This coincides with the main growing season for primary producers.

Recent work has shown that further changes have occurred in the lake sediment and factors regulating its behaviour. Generally, a larger mass of P is now released from the sediment each year than 30 years ago. The release of P is influenced by factors such as temperature, pH and nitrate concentrations. We have observed changes in these variables in Lough Neagh, especially since the 1990s, and these changes are likely influencing the mass of P released. The P released from the sediment in the summer can have negative water quality impacts and prevent the improvement of lake water quality that would otherwise have been apparent from nutrient management measures in the catchment.

This project quantified and characterised the sediment P in Lough Neagh and produced "timescales to recovery" models. Five cores were taken from the lake bed and sequentially analysed for different operationally defined P fractions. Each sediment core was also radiometrically dated. We used the P chemistry and dating information from the cores to derive an estimate of the time that it will take for the stored sediment P to be naturally removed from the lake. A model that included two major purging factors, diagenesis (transformation of particulate P to soluble P) and burial, provided a timescale of approximately 40 years. The model that used both purging factors was termed "the Full Model". These estimates of water quality recovery from internally loaded P will allow lake managers to take internally release P into account in setting their water quality targets. It is

important to note that the estimated timeframes provided by the models do not take into account continued catchment inputs to the lake, which must be continued to be managed responsibly.

Table of Contents

1.0) Introduction

Excessive input of anthropogenically derived nutrients has been identified as one of the key drivers of aquatic ecosystem degradation (Schindler 2006). This phenomenon of over-enrichment leading to rapid acceleration in primary productivity, known as cultural eutrophication, is widespread and has profound effects on within-lake ecosystem structure and functioning (Jeppesen et al. 2000; Schindler 2006).

At higher nutrient levels, algal blooms are common and the accompanying decline in water quality, including the increased risk of toxicity, oxygen stress and disease, leads to an overall reduction in water body amenity. Consequently, the global annual economic loss due to the increased costs of drinking water treatment, declines in fish biomass and reductions in recreational use has been estimated to be in the billions of US dollars (Smith and Schindler 2009).

Within Europe, one of the ways that eutrophication is being addressed is through the implementation of the Water Framework Directive (WFD) (European Commission 2000) (transposed into national legislation within in Northern Ireland through the Water Environment (Water Framework Directive) Regulations (Northern Ireland) 2017). The Directive intends for surface waters within member states to attain good ecological status (or potential) based on their extent of departure from defined reference conditions; i.e. an individual water body's degree of change from minimum disturbance conditions. Despite much effort in implementing monitoring and remediation programmes, only 53% of lakes in EU member states achieved good or better ecological status/potential at the end of the 2nd RBMP cycle (European Environment Agency 2018). Most lakes are subject to multiple pressures, any combination of which can cause a lake to fail to reach good status. Birk et al.

(2020) have highlighted that nutrient enrichment is the prominent stressor on European lake systems, which will be exacerbated by climate change.

Phosphorus (P) is often regarded as an important nutrient in lakes as it is commonly found to limit primary productivity due to its relatively low natural concentration in freshwaters (Schindler 1977; Schindler 2006). In particular, the strong associations identified between increasing water column total phosphorus (TP) concentration and shifts in lake ecosystem functioning (Jeppesen et al. 2000) means that in many cases P is utilised as a surrogate for lake productivity. As such, TP has become a frequently used metric for classifying lake trophic state and gauging the extent of eutrophication in standing waters (Vollenweider 1968; OECD 1982). Lake restoration efforts are often focused on the effective management of external P loading from point and diffuse sources to curb eutrophication. Most approaches are dependent on implementing improved catchment management measures/practices to reduce agricultural runoff, enhancing P recovery at wastewater treatment facilities, or if possible, the diversion of sewage discharges away from the waterbody (Foy et al. 1995; May et al. 2012).

It has long been known that controlling external inputs of P is essential to mitigate eutrophication and it must be emphasised that these measures are usually effective in bringing about an improvement in water quality (Vollenweider 1968; Schindler 1977; Jeppessen et al. 2005). However, a reduction in external loading does not always translate to an immediate decrease in lake water column P concentration, or recovery from unfavourable conditions. Several studies of lake recovery following external load reductions have encountered lag times on the scale of years to decades before any significant depletion of P and corresponding improvements in water quality are realised (Jeppessen et al. 2005; May et al. 2012; Søndergaard et al. 2013).

Delays in recovery often stem from internal P loading, the process whereby accumulated legacy P in lakebed sediment is recycled back to the overlaying water. This phenomenon buffers the lake response to a reduced external loading regime, effectively offsetting the progress of catchment based mitigation measures (Nürnberg 2009; Søndergaard et al. 2013).

The ability for lake sediments to switch between being a source and a sink of P has been well established in the literature, with the process leading to the release of soluble P reasonably well understood (Boström et al. 1988; Søndergaard et al. 2003). It is difficult to directly measure sediment P release from the lakebed as differing biological, chemical and physical influences often result in P uptake and release happening simultaneously. Instead, lake mass balances are calculated to determine net internal loading and its significance in regards to total P loadings (Nürnberg 2009). Net internal loading becomes more important in the summer months when lake flushing is decreased and temperature increases, often resulting in the supply of P from sediment becoming the dominant contributor to water column P (Søndergaard et al. 2013). This is true in Lough Neagh where mass balance calculations have identified mean summer internal load to be considerable and also increasing. From 1984 to 1994 the mean summer release of TP was 107 T and from 1996 to 2014 the mean TP release increased to 249 T (McElarney et al. 2021).

A primary cause for this year-on-year increase in TP release is due to increasing water temperatures brought about by climate change and the subsequent exacerbation of eutrophication within the Lough. This has substantial influences on the biological and redox sensitive sediment P stores. The well oxygenated surface sediments in Lough Neagh are expected to have a high capacity to retain P due to the affinity of P for metal oxyhydroxides and humic complexes under standard pH (Jensen and Andersen 1992; Ahlgren 2005; Hupfer and Lewandoski 2008). This oxygenated surface layer acts as a barrier to P in deeper anoxic sediment, thus facilitating the removal of legacy P from the system via burial (Søndergaard et

al. 2003). However, aerobic P release can occur when soluble P exceeds the retention capacity of the oxidised sediment layer (Jensen and Andersen 1992; Hupfer and Lewandoski 2008).

P release escalates during summer as temperature and biological activity increases in the organic matter rich sediments of Lough Neagh. Microbial activity increases the mineralisation of particulate P to soluble P, whilst consuming oxygen and reducing the thickness of the oxygenated layer. The presence of nitrate in the water column in early summer can often reduce release rates by maintaining oxygenation of the deeper sediments (Jensen and Andersen 1992). Although in Lough Neagh, the onset of nitrogen limitation in late spring likely diminishes the ability of nitrate to compensate for increased biological oxygen demand.

Additionally, heightened primary productivity in the overlying water column provides a ready supply of fresh organic matter to the lakebed, further stimulating biological activity (Søndergaard et al. 2003). As eutrophication progresses through summer, the excess primary productivity increases pH in the water column, further reducing the affinity of P for metal oxyhydroxides as the concentration of hydroxyl groups increases. With this, the remaining oxygenated sentiment can then loose a substantial capacity to capture solubilised P, facilitating P release to the water.

Lough Neagh is a naturally mesotrophic lake (medium enrichment, mean TP approximately 20 $\mu g\ L^{-1}$) but has become eutrophic due to a long history of nutrient loading (Battarbee 1978; Foy et al. 2003). Under the WFD, Lough Neagh is classified as a Heavily Modified Water Body (HMWB) due to ongoing water level regulation for flood risk reduction and to facilitate navigation. The water quality aim is to achieve Good Ecological Potential (GEP), however the Lough's highly enriched state means that it will be difficult to reach GEP in the

near future. In 2015, target TP concentrations set for 2021 were < 97 μg L^{-1} (Poor Ecological Potential; PEP), with the aim to achieve Moderate Ecological Potential (MEP), TP < 49 μg L^{-1}, by 2027 (objective setting currently under review (2020)). Attempts to substantially lower lake water TP concentration through control of catchment sources, have been unsuccessful (e.g. Foy et al. 1995); and mean annual TP was 139 μg L^{-1} in 2016. Water quality targets function as a benchmark to evaluate the success of the implemented restoration projects, yet the current targets do not account for any influence that the lake sediment has on the water quality in Lough Neagh. As the internal load is known to be significant in Lough Neagh (Gibson et al. 2001), it is critical to further understand the extent of the historically accumulated sediment P in order to predict when and how the lake will respond to changes in external loading (Penn et al. 1995; Lewis et al. 2007).

The main objective of this work was to quantify and characterise the P pool within Lough Neagh sediment, and utilising a sediment P model, construct a timescale to recovery from P eutrophication. Here recovery is defined as the point where the internal P load diminishes to an insignificant amount and reaches steady state with overlaying water column, i.e. when sediment P release will be in equilibrium with P uptake. This will help guide lake managers to define alternative, realistic targets that reflect the delay in recovery caused by the supply of P from internal loading. We also characterised the lake sediment in terms of P content and presence of different operationally defined forms of P.

2.0) Methods

2.1 Site Description

Lough Neagh is a large lake situated in the north-east of the island of Ireland with a surface area of 383 km^2, volume of 3.45 km^3, and hydraulic residence time of approximately 1.3 years. Eight major tributaries discharge into the Lough from the 4,453 km^2 catchment basin, and the outflow, the Lower Bann, drains north to the Atlantic Ocean (Wood and Smith 1993). Water levels are maintained via sluice gates at Toome (at the entrance to the Lower Bann) to be within a range of 12.45-12.60 m O.D. Belfast as specified in the Lough Neagh Levels Scheme (1955).

The Lough is polymictic with a well-mixed water column throughout the year (mean depth 8.9 m), high mean wind speeds (~5m s^{-1}) and large effective fetch (max = 17.7 km). However, brief periods of stratification can occasionally occur during summer months when exceptionally calm weather (persistent mean wind speeds < 2m s^{-1}) allow for the formation of a thermal gradient in the water column (Wood and Smith 1993).

The Lough is a critical drinking water supply for the population of Northern Ireland, with three water treatment works located on its shores licensed to abstract a combined total of 392 Ml d^{-1}, over a third of the total licensed abstraction volume of raw water for Northern Ireland – 1075 Ml d^{-1} (NI Water 2012). The Lough sustains an economically significant fishery which, in addition to scale fishing, lands 400 – 600 tonnes of the critically endangered European Eel (*Anguilla anguilla*, Linnaeus 1758) (IUCN Red List species) per annum worth circa £3 million to the Northern Ireland economy.

Lough Neagh is designated locally as an Area of Special Scientific Interest (ASSI) and a wetland of international importance under the Ramsar Convention for supporting diverse assemblages of wildfowl. The site also qualifies based on its selection of rare or vulnerable

species, most notably Pollan (*Coregonus autumnalis*, Pallas 1776), a fish species endemic to Ireland (listed as a UK priority species; Irish Red Data Book endangered species; and on Annex V of the EU Habitats Directive (European Commission 1992). Moreover, the site has gained designation as a Special Protection Area under European Directive 2009/147/EC (European Commission 2009) on the grounds of supporting assemblages of nationally and internationally important overwintering and breeding wildfowl.

2.2 Sample Collection

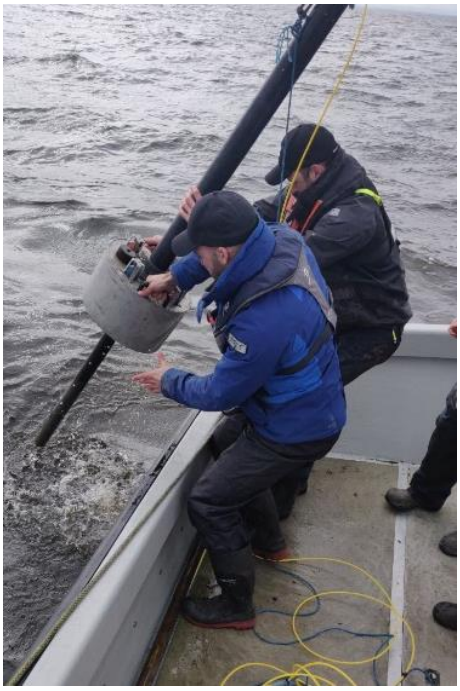

Five sediment cores were retrieved from Lough Neagh between December 2018 and April 2019 using a 1 m mini-Mackereth pneumatic piston corer (Mackereth 1969). All 5 core samples were collected from depths between 10-13 m (Figure 1) where muddy profundal sediments form an almost uniform flat bed. Although almost the entire lake bed experiences disturbances (Battarbee 1978; Wood and Smith 1993), the generally lower energy depositional environment at these depths offered a better representation of the long term P accumulation, and provided a higher probability of recovering an intact sediment profile (Rowan et al. 1995).

Previous sediment coring has identified temporal and spatial variations in sediment accumulation rates within the flat depositional area (Battarbee 1978), likely owing to regular wind-driven resuspension and redistribution of bed sediment (Battarbee 1978; Douglas and Rippey 2000). Consequently, the five sites were distributed to provide sufficient accuracy in

estimating whole lake sediment P accumulation, whilst accounting for spatial variations that may exist (Fletcher 1990; Rowan et al.1995) (Figure 1).

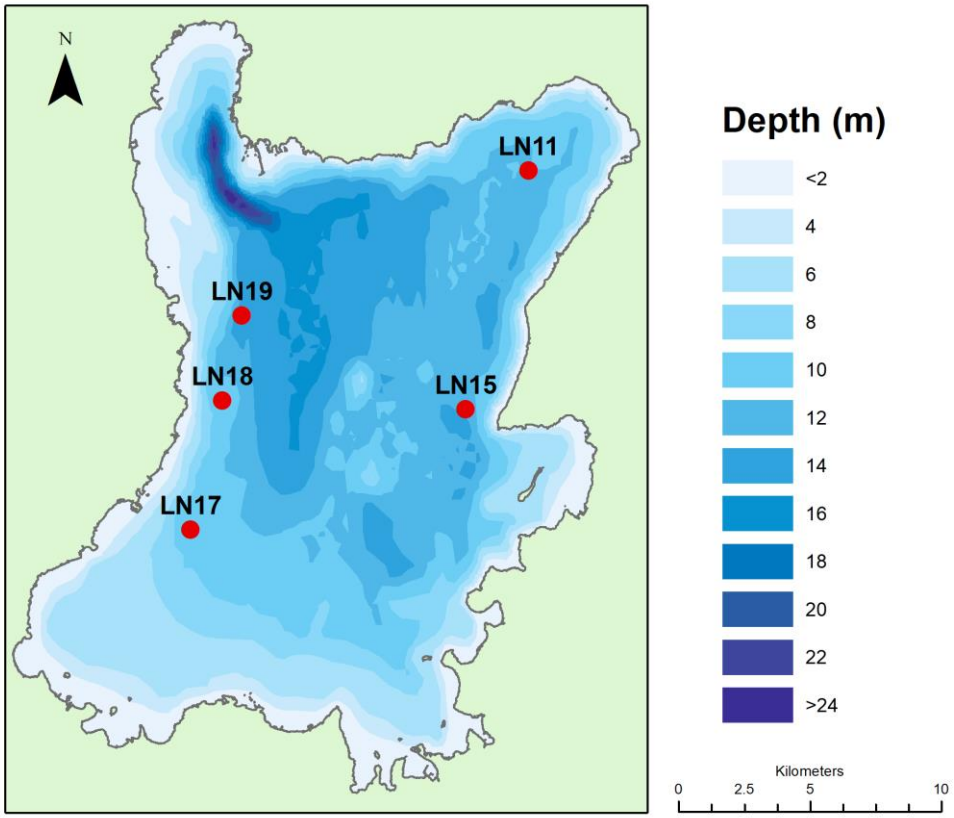

Figure 1: Bathymetric chart of Lough Neagh. Sediment coring locations are symbolised by the circles.

Once retrieved, the cores were inspected to ensure a clearly defined sediment-water interface was present. Any samples displaying evidence of disturbance were disposed of and another sample attempted. Successful cores were sealed and immediately transported to the lab where they were stored vertically at 4^{o} C until extruded.

2.3 Core Extrusion

The sediment cores were extruded and sectioned at 1cm intervals until 30 cm, and then 2 cm intervals thereafter until the core was fully extruded. Wet sediment was immediately transferred to polypropylene containers and the headspace purged with nitrogen to prevent oxidation of anoxic sediments whilst stored at 4^{o} C. Shielding with nitrogen preserved the sediment by limiting storage induced changes in the redox sensitive P fractions, prolonging the stability of samples to approximately 26 days (Lukkari et al. 2007a). The extraction procedure usually began within 24 hours, and was completed within one week from the date of extrusion.

2.4 Determination of sediment P forms

A variety of organic and inorganic P forms occur within lake sediments, some are more susceptible to recycling and release. It is therefore necessary to characterise the different forms of sediment P to identify the proportion of TP that is bioavailable (labile) from those forms that are more stable (refractory) (Lukkari et al. 2007b).

As described in Penn et al. (1995), a 1.5 g subsample of wet sediment was taken from each slice of extruded core sample and subjected to the P extraction scheme laid out in Figure 2, with manual shaking of the samples taking place at regular intervals during the extraction procedure. The extraction scheme followed that described by Heiltjes and Lijklema (1980), with an additional separation of reactive and non-reactive P from the NaOH step conducted to improve the characterisation of the NaOH extract (Furumai and Ohgaki 1982). A series of reagents (NH_4Cl, NaOH, HCl) were used to sequentially extract different phosphorus species which were defined based on their solubility in or reactivity with the solutions with increasing strength (Lukkari et al. 2007b), making it possible to categorise P forms as either

labile or refractory. When each step was complete the extracts were centrifuged at 4,500 rotations per minute for 30 minutes; the resulting supernatant was poured off and then filtered through a 0.45 μm filter before the next reagent being added.

For the final step, any recalcitrant residual-P was extracted using the ignition method as described in Ostrofsky (2012), a modified version of Andersen (1976). The extract was then transferred into a 50 ml volumetric flask and diluted to the line with deionised water.

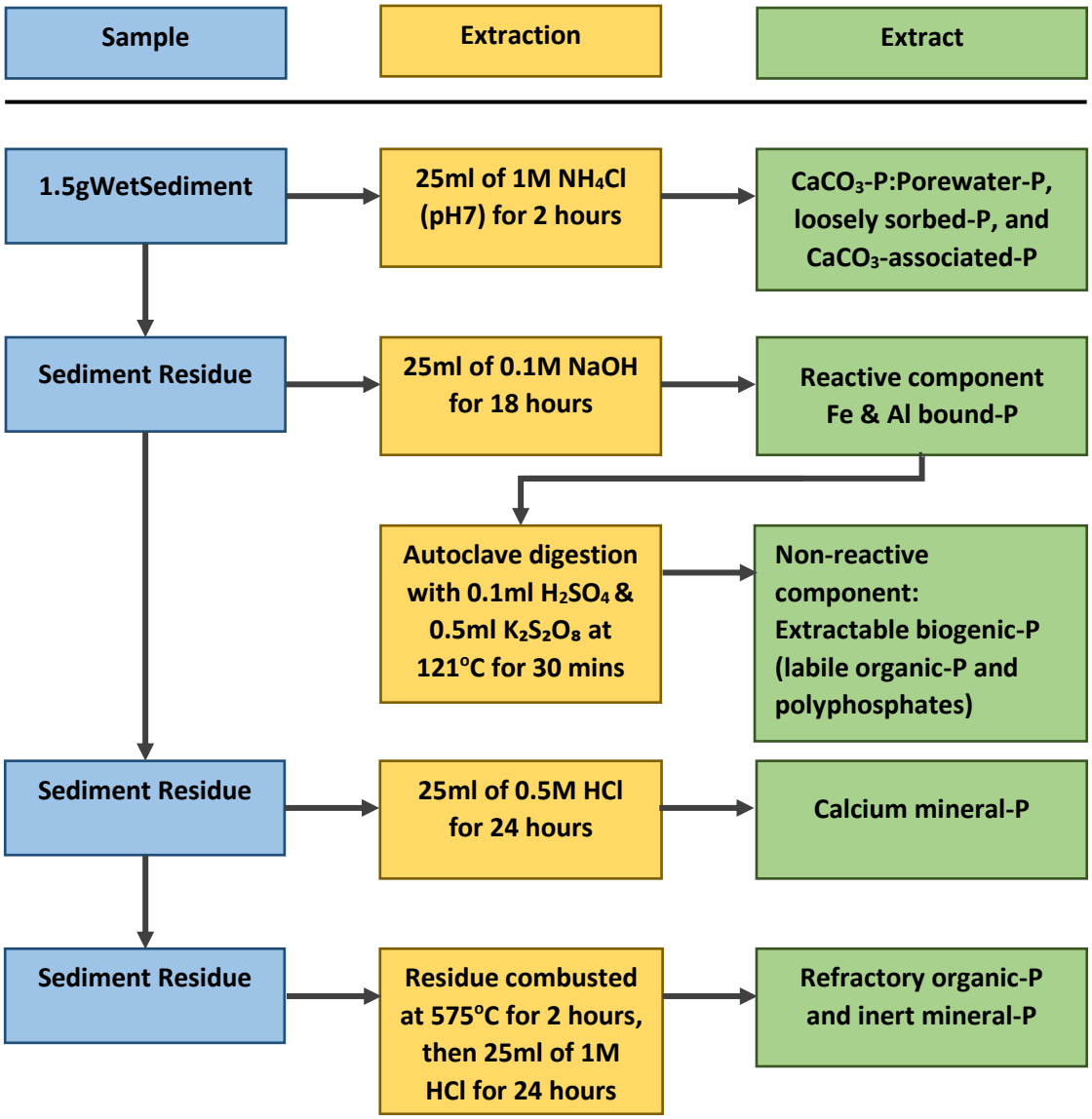

Figure 2: Protocol for extracting operationally defined P fractions as defined by Penn et al. (1995).

The concentration of soluble reactive phosphorus (SRP) in the filtered extracts was determined photometrically as described by Murphy and Riley (1962). Total Soluble Phosphorus (TSP) concentration of the NaOH extract was determined following digestion with sulphuric acid and potassium persulphate at 121 ^{o}C for 30 minutes (Eisenreich et al. 1975). The concentration of the non-reactive component of the extract was calculated as the difference between $NaOH_{TSP}$ - $NaOH_{SRP}$.

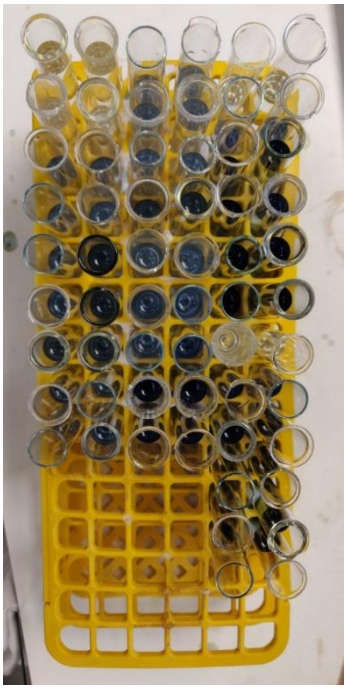

Excluding NH_4Cl, all extracts were diluted twentyfold to ensure the concentration of P in solution was within the linear range of the P determination method, and were neutralised to bring the pH the extracts into the optimal range for the method. The absorbance of the final solution was read at 880 nm using an Aquakem 250 Discrete Photometric Analyser (ThermoFisher Scientific) against a calibration curve generated from an array of P standards.

2.5 Basic sediment characteristics

Wet sediment density was determined from the weight of known volumes of sectioned wet core sediment using the covered calibrated slice method of Hilton et al. (1986). Dry mass was quantified gravimetrically as the difference between sediment wet weight and weight following drying at 105 ^{o}C for 24 hours. Loss in mass was recorded and then used to calculate the remaining dry weight as a percentage of wet weight.

Dried sediment was then lightly ground and homogenised. A subsample (approximately 1 g) was combusted for two hours at 550 ^{o}C in a muffle furnace. The sample was then reweighed to calculate percentage loss on ignition as an estimate of organic matter content as weight loss is proportional to the amount of carbon present in the sample. The remaining ash was

again combusted at 1000 ºC for one hour, and loss in weight used to ascertain carbonate content (Dean 1974).

2.6 Sediment chronology

The radiometric dating used to construct sediment chronologies was performed by the University College London Environmental Research Centre. The radionuclides ^{210}Pb, ^{226}Ra, ^{137}Cs, and ^{241}Am within the core sediments were measured by direct gamma assay using an ORTEC HPGe GWL series well-type coaxial low background intrinsic germanium detector (Appleby et al. 1986; Appleby et al. 1992).

^{210}Pb has a half-life of 22.3 years and is effective for dating sediments to over 100 years. It enters lake sediments via two main pathways; as supported ^{210}Pb – the product of in situ ^{226}Ra decay, and unsupported ^{210}Pb via atmospheric deposition. Unsupported ^{210}Pb activity is highest at the surface sediments due to more recent inputs and activity usually diminishes moving down the core. The supported component was assumed to be in equilibrium with its parent isotope ^{226}Ra, allowing for the atmospheric flux (unsupported) to be determined from the difference between total ^{210}Pb activity and supported activity at each depth (Appleby and Oldfield 1978; Appleby 2001).

^{210}Pb chronologies were calculated using the constant rate of ^{210}Pb supply (CRS) dating model (Appleby and Oldfield 1978). This model assumes the atmospheric flux of ^{210}Pb is a constant rate and that all unsupported activity in sediments is due to inputs from atmospheric deposition. These assumptions made the model suitable for sediments prone to disturbances and/or with variable sediment accumulation rates (Appleby 2001). Sedimentation rates for each core were calculated via liner interpolation of the age-depth model. The model was supplemented by measuring activity of the artificial radionuclides ^{137}Cs (half-life is 30 years) and ^{241}Am (half-life 432 years), deposited to the sediments following atmospheric fallout from nuclear reactor accidents (1986) and peak nuclear weapons testing (ca. 1963) (Appleby 2001).

2.7 Lake sediment model overview

Diagenesis of P is the transformation of particulate P to dissolved soluble P. The model we present can be separated into two main components; the calculation of a diagenetic rate from the model proposed by Penn et al. (1995) (the Foundation Model) and the condensed box model suggested by Lewis et al. (2007) (the Full Model). The latter model builds on the Foundation Model and gives a more complete estimate for the timescale of recovery in Lough Neagh.

Steps in applying the models are described in more detail within sections below. In summary, the Full Model estimates time taken for lake sediments to respond to a reduced loading regime based on two dominant purging factors (Lewis et al. 2007). Within this condensed continuously stirred tank reactor model the purging factors are summarised as rate of P loss through chemical transformation and release (diagenesis rate, k_d yr^{-1}) and the burial rate (ω cm yr^{-1}) of P from the active layer (Z_{active} cm) as described in Chapra (2008). Here the

active layer is defined as the zone where labile particulate P undergoes diagenesis, and is subsequently released to the water column (Lewis et al. 2007).

The models treat each 1-2 cm section of the sediment core profile as a distinct layer and the extent of P transformation within each layer is calculated (Penn et al. 1995). The degree of P diagenesis moving down the core profile from the sediment-water interface (SWI) is then used to establish the rate of labile P recycling. Burial represents the downward rate of movement of each section/slice with respect to the sediment surface, whereby the continuous deposition of sediments forces each section away from the SWI and eventually out of the active layer (Lewis et al. 2007; Chapra 2008).

3.0) Results and Discussion

Results are presented alongside figures from core LN18 for illustration. Full results and figures for the remaining four core samples are provided in the Appendix.

3.1 Radiometric Dating

Aside from LN18 (Figure 3), all cores display peak ^{210}Pb activities below the sediment surface (peak range 124.99 – 97.81 Bq Kg^{-1}). Unsupported ^{210}Pb activity, i.e. excess to that derived from the natural decay of ^{226}Ra, is assumed to originate from atmospheric fallout depositing ^{210}Pb to the lake at a constant rate. Thus, elevated concentrations of unsupported ^{210}Pb below the surface indicates dilution of the annual atmospheric flux due to an increase in sedimentation rate within recent years (Appleby 2001).

Alternatively, elevated ^{210}Pb below the surface may suggest interference from sediment mixing at the surface facilitating the downward movement of ^{210}Pb activity, which would result in an overestimation of contemporary sediment accumulation (Bachmann et al. 2018). Vertical mixing of the upper sediments is common in Lough Neagh due to regular disturbances from wind induced turbulence at the SWI (Douglas and Rippey 2000) and bioturbation/bio-irrigation from high chironomid densities (Carter and Murphy 1993). The use of a CRS (constant rate supply) model with additional artificial radionuclides profiles improves the reliability of the ^{210}Pb age-depth model in providing long-term chronology required for this study (Appleby 2001).

The depths at which total ^{210}Pb activity reached equilibrium with supported ^{210}Pb activity ranged from 16 cm (LN19) – 55 cm (LN15), with all cores showing irregular non-monotonic declines in unsupported ^{210}Pb activities with depth. LN11, LN15, and LN17 display more variable fluctuating profiles than LN18, and especially more irregular than LN19, which in

comparison presents a gently sloping ^{210}Pb profile (Appendix Figures 1; 6; 11; 16). These differences both within and between cores suggest variations in sedimentation rates over both time and space within the Lough.

Two areas of interest were between 8 – 12 cm in core LN11, and 16 – 28 cm in core LN15, where uncharacteristic declines in unsupported ^{210}Pb implied increased sedimentation at these depths (Appendix Figures 1 and 2; 6 and 7). Figure 3 below displays the unsupported ^{210}Pb activity, ^{137}Cs and ^{241}Am activity for core LN18. Figure 4 below shows the resulting CRS dating model output for core LN18, with sediment mass accumulation rate in g cm^2 yr^{-1}.

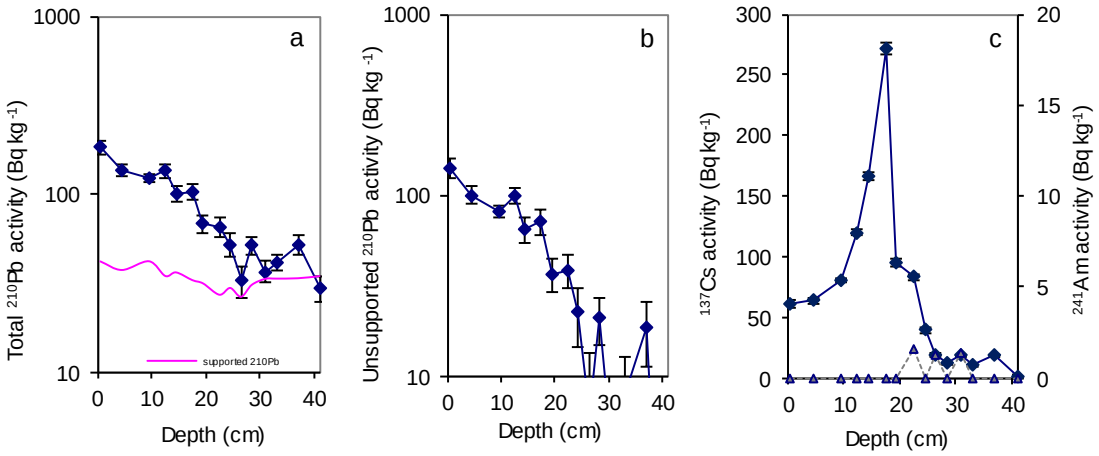

Figure 3: Fallout radionuclide concentrations, as provided by UCL ERC, in core LN18 taken from Lough Neagh, showing (a) total ^{210}Pb, (b) unsupported ^{210}Pb, and (c) ^{137}Cs and ^{241}Am concentrations versus depth.

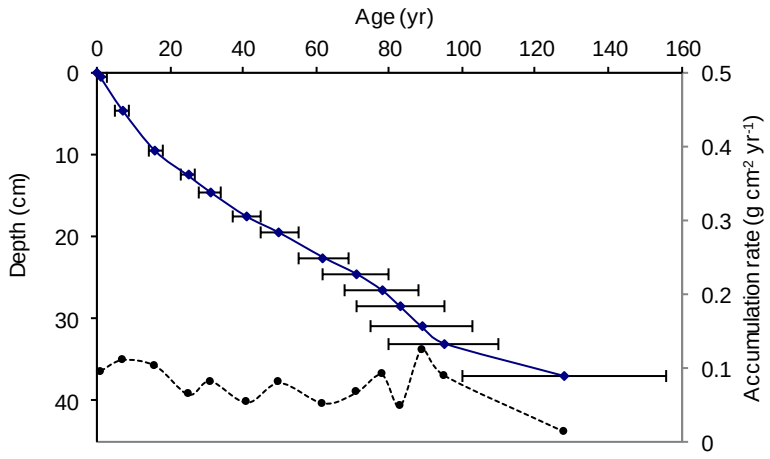

Figure 4: Radiometric chronology of core LN18, showing the CRS model ^{210}Pb dates and sedimentation rates. The solid line shows age while the dashed line indicates sedimentation rate.

CRS models established core chronologies up to a maximum ca. 150 years. The models reach a base dateable region ranging from 1916 in core LN11 at 16 cm, to 1867 in core LN17 at 29 cm. Pronounced peaks in ^{137}Cs activity, signifying the 1986 Chernobyl disaster, occurred at depths ranging from 7 cm (LN19) – 18 cm (LN18). These dates were in reasonable agreement with the placement of 1986 by the CRS models, validating the models effectiveness in providing a reliable chronology. Measured ^{241}Am, signalling the height of nuclear weapons testing in 1963, was detectable at depths of 8 – 24 cm, however it was often detected in insufficient quantities for dating, either as a single point in the profile or being obscured by the 1986 ^{137}Cs activities.

The maximum sediment mass accumulation rate (MAR) was identified by the CRS models at the surface of core LN19, which then followed a gradual decrease from higher recent accumulation to its minimum MAR at 13 cm (range 0.0062-0.0376 g cm^{-2} yr^{-1}). LN11, LN15, and LN17 experienced abrupt, off-trend fluctuations in mass accumulation at depth, peaks were found at 9.5 cm (1975), 27.5 cm (1966), and 16.5 cm (1963), corresponding to dates of 1975, 1966, and 1963 (Appendix Figures 2; 7; 12). Maximum accumulation within

these cores ranged from 0.164 cm^{-2} yr^{-1} in LN17 to 0.0106 g cm^{-2} yr^{-1} in LN11. LN18, displayed in Figure 4, also experienced an unusual off-trend peak (0.125 g cm^{-2} yr^{-1}) at 31 cm, equivalent to a date of 1929. Minimum MAR between 0.0062 – 0.0265 g cm^{-2} yr^{-1} generally occurred at the base region covered by the CRS models; between 1867 – 1903.

3.2 Basic sediment characteristics

Decades of external loading has resulted in the TP within sediments (e.g. LN18 presented in Figure 4; Appendix Figures 3, 8, 13, 18 for remaining cores) being a magnitude higher than the concentration of TP in the overlaying water column. LN17 had both the largest and smallest measured TP concentration of all cores (range 0.49 – 3.37 mg gDS^{-1}), whilst LN19 had the smallest range (0.75 – 1.19 mg gDS^{-1}). There appears to be a degree of spatial variation in both sediment TP concentration and the shape of TP profile. LN15, LN17, and LN18 had similar surface (0-1 cm) concentrations of 3.17 – 3.48 mg gDS^{-1} and exhibited similar sloping TP profiles with depth. LN11 and LN15 varied with surface concentrations of 2.54 and 1.94 mg gDS^{-1} respectively. LN19 had a more shallow profile while LN11 appeared to have rapidly diminishing TP within the first approximately 5 cm before following a profile similar to LN19.

Dry weight as a percentage of wet sediment, represented mean ± SE of 22.9 ± 1.66 % WS weight. Dry weight typically increased with depth in all cores, fluctuating from 9.0 % WS at LN15 surface to 23.58 % WS at 45 cm. The greatest dry weight was found at 41 cm LN17 to be 39.13 % WS. Increases of dry weight with depth suggest a shift towards higher mineral content down through the sediments.

Loss on ignition (LOI) as a percentage of dry weight followed a more consistent, inverse trend of % dry weight. LOI generally decreased with depth in all cores, suggesting a

decrease in sediment organic material with depth. Maximum LOI reached 21.59 % at the surface layer of LN15 and declined to 11.65 % at 45 cm. The lowest observed LOI value was found to be 6.84 % at 41 cm LN17. Overall, mean ± SE for the five cores was 13.65 ± 0.75 % DS weight.

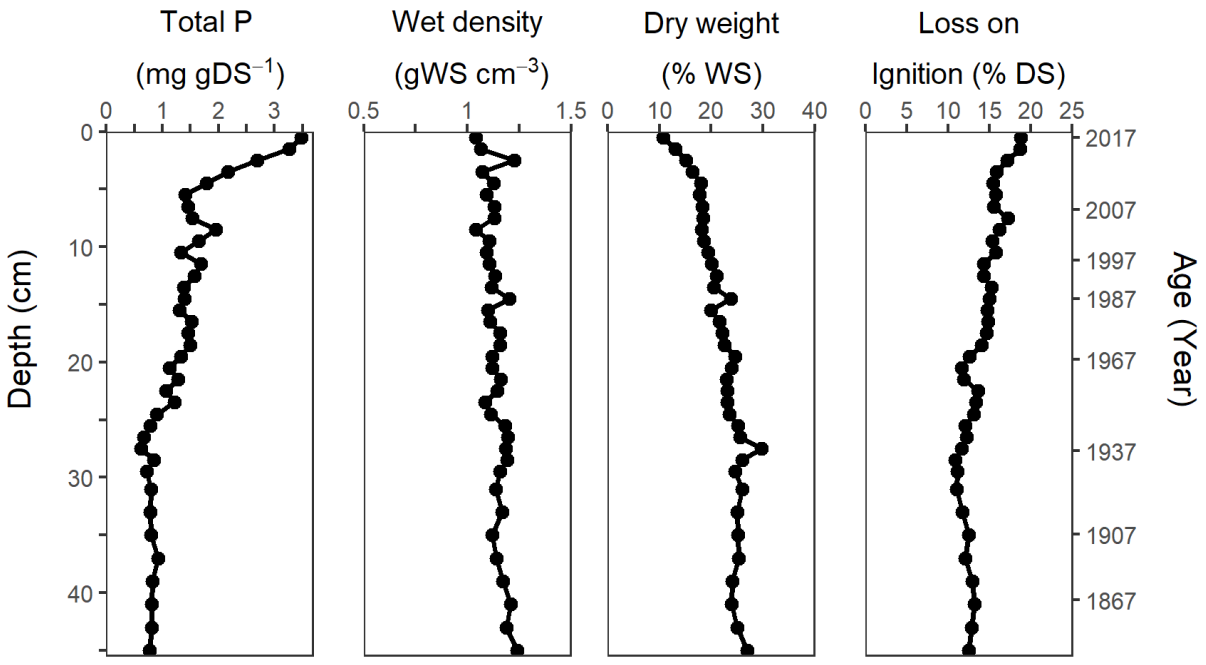

Figure 5: Basic sediment overview for core LN18 to 45 cm. Total phosphorus, wet density, dry weight as a percentage of wet weight, and loss on ignition (proxy for organic matter content) as a percentage of dry sediment weight. Sediment age on the secondary y-axis obtained from ^{210}Pb CRS model chronologies until 37 cm (1890) and extrapolated until 45 cm.

When grouping all samples together, it is clear that DW and LOI are intrinsically linked. A significant negative correlation was present between the parameters with LOI decreasing with increasing DW ($R = -0.92$, $n = 190$, $p<0.001$, with a $R^2 = 0.85$). Both DW and LOI display weaker, yet still significant, correlations with TP in sediments, with TP decreasing as DW increases ($R = -0.75$, $n = 190$, $p<0.001$, with a $R^2 = 0.57$), and TP increasing with increasing

LOI ($R = 0.74$, $n = 190$, $p<0.001$, with a $R^2 = 0.55$). The strong relationship between these three parameters can be attributed to the decay of organic matter when moving downwards from the SWI. Within surface sediments, low dry weight with higher LOI and TP (e.g. in the upper 5 cm of core LN18, Figure 5) suggests the presence of relatively unconsolidated surface sediment with elevated microbial/biological activity. Furthermore the high organic and water content makes the surface sediment susceptible to resuspension (Douglas and Rippey 2000).

Large shifts towards increased dry weight at depth could imply dilution with allochthonous (catchment based) minerals sourced from catchment erosion, or the re-deposition of mineral material from the erosional littoral area within the lake (Battarbee 1978). For LN15, an atypical shift in LOI, DW, and to a smaller extent, TP, occur between 9 cm and 17 cm implies a potential change in sediment structure.

There was comparatively little variation in wet density, both within and between cores. Mean ± SE wet density was 1.13 ± 0.02 gWS cm^{-3} with a range of 0.97 – 1.3 g cm^{-3} when excluding the one atypical value from LN17 surface (0.58 g WS cm^{-3}). Wet density exhibited weaker relationships with the other parameters: WD vs TP ($R = -0.41$, $n = 190$, $p<0.001$, with a $R^2 = 0.17$); WD vs DW ($R = 0.47$, $n = 190$, $p<0.001$, with a $R^2 = 0.22$); WD vs LOI ($R = -0.41$, $n = 190$, $p<0.001$, with a $R^2 = 0.17$). Wet density generally increased with depth as sediment compaction increased and composition changed from unconsolidated sediment at the SWI, then fine mud, until reaching clays deeper in the profile.

Additionally, measured carbonate in sediments (Figures not shown here), was consistently <3% dry weight in all core sediments and was found to have no significant relationship with P or any of the above measured physical characteristics.

3.3 Phosphorus fractions

The variation of sediment phosphorus fractions for core LN18 over both depth and time is shown in Figure 6 (see Appendix Figures 4, 9, 14, 19 for P fraction profiles for remaining cores). Total P decreased with depth until reaching a stabilisation point but not all fractions were present in equal concentrations, nor did they diminish equally. For LN18 (Figure 6) in particular, the order of fractions in terms of contribution to total extracted P at the surface layer (0-1 cm) were as follows NaOH-SRP >HCl-P > Residual-P >NaOH-NRP > NH4Cl-P shifting to Residual-P >HCl-P >NaOH-SRP >NaOH-NRP > NH4Cl-P below 24 cm, remaining fairly constant with depth.

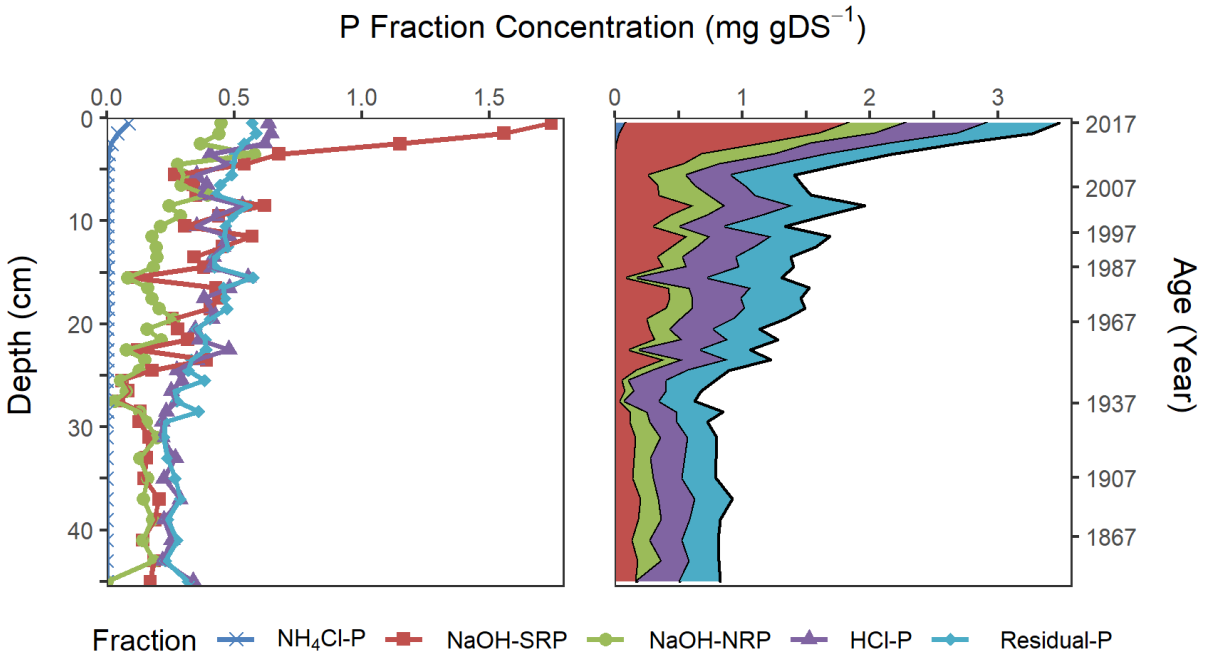

Figure 6: Vertical profiles of extracted P fractions in core LN18 in mg gDS^{-1} until 45cm. For clearer interpretation, variations in P fraction concentration is displayed both individually (left) and stackable area (right). The sum of the 5 fractions is equivalent to total extracted P. Sediment age on the secondary y-axis obtained from 210Pb CRS model chronologies until 37 cm (1890) and extrapolated until 45 cm.

Within all core sediments, NH_4Cl or 'loosely bound-P', was by far the smallest P pool and was practically non-existent beneath 5 cm depth. A peak concentration of 0.085 mg g^{-1} DS was detected in the surface sediments of LN18, still exceptionally low in comparison to other P fractions, and contributing only 2.4% of TP in that 0-1 cm sediment layer. This fraction represents the most readily available forms of P existing in the sediment pore water, and its restriction to surface sediments suggests that it is the product of both upwards diffusion of soluble P from deeper sediments and ongoing mobilisation of P at the surface. In aerobic sediment with high iron content, such as that of Lough Neagh, recently mobilised P often adsorbs to iron oxyhydroxides (NaOH-SRP/Fe-P), so the presence loose pore water-P at surface sediments only may indicate that P binding sites are at capacity (Boström 1988; Hupfer and Lewandoski 2008).

The largest P fraction within surface sediments (0-1 cm) was the NaOH-SRP fraction (reactive Fe and Al bound-P), with a mean concentration of 1.2 mg gDS^{-1} (range 0.78 – 1.75 mg gDS^{-1}), and a maximum concentration beneath the surface (1-2 cm) of 1.79 mg gDS^{-1} in LN17. Fe-P is the largest fraction in the surface sediments of the collected core samples as it is a typical feature of Lough Neagh sediment (Fletcher 1990; Rippey 1980), and previous work has highlighted the significance of iron mediated seasonal P release in Lough Neagh (Gibson et al. 2001). Despite dominating the surface sediments, the reactive NaOH fraction exhibited the most erratic vertical distribution with fluctuating steep declines, this fraction became one of the least represented fractions by the stabilisation point marking the active layer depth. By the 45 cm mark, the deepest point analysed for sediment P, NaOH-SRP had a mean concentration of 0.147 mg gDS^{-1} (range 0.076 – 0.186 mg gDS^{-1}), an overall decline of 88 % and a shift in mean relative TP contribution from 42 % to 19 %.

NaOH-NRP (non-reactive biogenic-P) displayed a similar, but less extreme, declining trend with a smaller overall range of 0.652 – 0.031 mg g^{-1} DS (excluding the possible error value of

0 mg g^{-1} DS value for LN18 45 cm, which was most likely the result of incomplete extraction as indicated by the coinciding increase in HCl-P and Residual-P; Figure 6). In spite of its declining concentration, the fraction's mean relative contribution to total extracted P increased slightly from approximately 18 % at surface layers to 21 % at 45 cm. From this it can be assumed that NaOH-NRP is sensitive to decay, but less so than NaOH-SRP, and may contain P forms that are resistant to transformation which would facilitate it's preservation with depth (Penn at al. 1995; Rydin et al. 2000).

Mean concentration of both HCl-P (calcium mineral-P) and Residual-P (inert mineral-P and recalcitrant organic-P) were least variable/most stable in core profiles, with smaller declines in mean concentrations. HCl-P concentration declined from 0.518 mg gDS^{-1} (range 0.634 – 0.323) at surface to 0.237 mg gDS^{-1} (range 0.338 – 0.170) at 45 cm. Similarly, Residual-P declined from 0.516 mg gDS^{-1} (range 0.862 – 0.429) at surface, to 0.259 mg gDS^{-1} (range 0.319 – 0.180) at 45 cm. These two P forms are resistant to change and persist in the sediment, unable to participate in the recycling of P back to the overlaying water (Penn et al. 1995). The relative contribution of HCl-P and Residual-P to TP increased by approximately 30% with depth as other P forms experienced more significant declines in concentration.

It is clear that the different P forms liberated during the extraction procedure have varying potentials for mineralisation and recycling. The following section (3.4) shows how we classified sediment P based on its availability for contribution to internal loading.

3.4 Determination of labile P in sediment

Penn et al. (1995) proposed that the sediment P inventory can initially be divided into two main categories:

- Fraction A – the labile or bioavailable fraction – P species available for transformation and recycling back to the water column.
- Fraction B – the refractory or inert fraction – unavailable for diagenesis, locked in sediment

The authors suggest that Fraction A consists of the sum of pore water and CaCO3-P, Fe & Al-P, and extractable biogenic-P (sum of NH_4Cl-P, NaOH-SRP, NaOH-NRP), whilst Fraction B consists of the remaining two forms, Ca mineral-P, and residual-P (sum of HCl-P and Residual-P).

Within the Lough Neagh cores, Fraction A experienced the greatest range of P concentration (0.077 – 2.39 mg gDS^{-1}). High surface concentrations decreased substantially with depth until reaching a stabilisation point, following which, Fraction A concentration then remained relatively constant down the sediment profile. This stabilisation point marked the base of the active layer (Z_{active}), the zone where the bulk of diagenesis occurs. Fraction A often reduced its contribution to TP by approximately 20 % with depth, primarily due to fluctuations in NaOH-SRP. As NaOH-SRP was often the largest component of Fraction A, its wide fluctuations contributed to the irregular vertical distribution seen in Figure 7. Fraction B on the other hand displayed a more regular decreasing trend in its vertical distribution, with ranges of 0.305 – 1.48 mg gDS^{-1}.

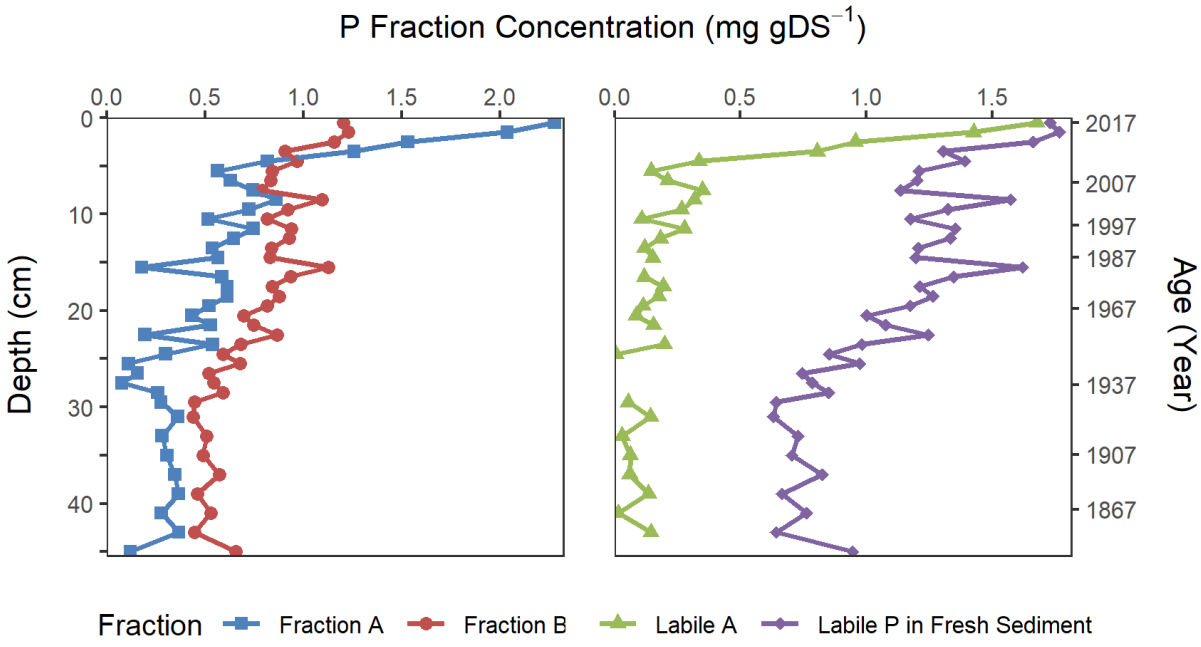

Figure 7: Left displays vertical profiles of Fraction A (sum of NH_4Cl; NaOH-SRP; NaOH-NRP) and Fraction B (sum of HCl-P; Residual-P) in core LN18 in mg gDS^{-1} until 45 cm. Right displays profile of Labile A (bioavailable-P) present in the sediment at time of analysis and Labile P at time of deposition to sediment surface. Sediment age on the secondary y-axis obtained from ^{210}Pb CRS model chronologies until 37 cm (1890) and extrapolated until 45 cm.

Beneath the active layer of each core it was assumed that diagenesis had, for the most part, ceased and any remaining P was considered inert and unavailable for transformation. Nonetheless, Fraction A on average still contributed to 40 % of TP below Z_{active} (Figure 7, left) implying that a refractory component existed within Fraction A. Thus, to ascertain the concentration of genuinely labile P it was necessary to subtract the refractory component, Refractory A, from Fraction A.

It was not possible to apply a single correction to eliminate Refractory A from the sediment P profile due to the inconsistent rate of P deposition over time. Instead, equation 1 was used to adjust the concentrations at each depth down the core profile. The equation utilised Fraction

B as point of reference to gauge the extent of labile P diagenesis as refractory P was expected to remain comparatively stable from time of deposition.

The ratio between remaining Fraction A to Fraction B below Z_{active} was calculated and used to estimate the proportion of Refractory A at each depth. The refractory component, Refractory A, was then subtracted from the chemically extracted Fraction A at each depth to provide the truly labile component of the Fraction A inventory, termed Labile A (Figure 7, right):

$$FA_{rz} = \alpha\, FB_z$$

$$LabA_z = FA_z - FA_{rz} \quad (1)$$

Where FA_{rz} is the refractory component of Fraction A at a certain depth (z); α is the ratio between Fraction A and Fraction B below Z_{active}; FB_z is the mass of Fraction B at a certain depth (z) determined by chemical extraction; FA_z is the mass of Fraction A at a certain depth (z) determined by chemical extraction; $LabA_z$ is the calculated mass of truly labile Fraction A at a certain depth (z).

Total Refractory P inventory at each depth ($RefP_z$) was then calculated as the sum of measured Fraction B and the refractory component of Fraction A at each depth (equation 2):

$$RefP_z = FB_z + FA_{rz} \quad (2)$$

Penn et al. (1995) provided a ratio (r) for labile P to refractory P in fresh sediment at time of deposition. This was based on observed concentrations from sediment traps deployed in their study lake, and assumed the ratio of 49 % labile P to 51 % refractory, r = 0.96, which remained constant over time. Using this ratio it was then possible to calculate the estimated labile content in fresh sediments P at initial deposition to the lake bed (P_{L0}) using equation 3:

$$P_{L0} = RefP_z \cdot r \quad (3)$$

The r-value in equation 3 is lake specific, depending on both catchment (land use, geology) and within lake characteristics, e.g. trophic state, morphology. The model employed the same calculation/ratio at each depth, however, it did not have an effect on the final diagenesis rate constant. That is instead controlled by the measured refractory P inventory, which persists in the sediment following deposition.

Figure 7 (right) shows the transformation of labile P in core LN18 with depth. Labile P in fresh sediment is the predicted concentration of P available for diagenesis at time of initial deposition to the lakebed, and Labile A represents the measured labile P remaining in the sediment. Therefore, the difference between the two profiles illustrates the extent of through core diagenesis. There was very little variance at the surface, but it was clear that rapid mineralisation occurred in the first 5 cm from the SWI. Labile P transformation then continued with depth, albeit considerably more slowly.

A notable interruption in the Labile A trend occurred in LN15 between 9 -17 cm, this resulted in a gap in calculated labile P within the active layer. This was unusual in comparison to

other collected core samples, although this section of the core profile with reduced labile P coincided with a sudden fall in net sedimentation as identified by radiometric dating, and an uncharacteristic shift to a higher mineral content with a decrease in LOI and increase in sediment dry weight (Appendix Figure 10, 8).

In comparison, with the exception of occasional fluctuations (e.g. LN11 7 - 8 cm) cores LN11, 17, 18 and 19 (Appendix 5, 15, 20) had reasonably relatively well defined profiles of Fraction A and Labile A, uninterrupted by any significant disturbance. Core LN18 experienced multiple discrete abnormalities in the15 cm, 22 cm, and 25-27 cm regions. These fluctuations from the trend had very little effect on the final diagenetic rates (and recovery rates), but demonstrate the variability of labile P forms.

3.5 Estimating timescales to recovery

3.5.1 Purging factor 1 - Diagenesis rates (the Foundation Model)

P diagenesis is commonly understood to follow a first order rate, whereby particulate P within sediments is mineralised, or transformed, exponentially over time. The decay rate coefficient (k_d) can be derived via the slope from a log-linear regression of the ratio between estimated labile P at time of sampling (P_{Lt}) and labile P at initial deposition (P_{L0}) against time in years (t). This forms the basis of the Foundation Model (Figure 8), describing the long term flux of P, and can be expressed by equation 4:

$$-ln\frac{P_{Lt}}{P_{L0}} = k_d.t \quad (4)$$

Penn et al. (1995) identified a fast and slow diagenetic rate in the sediments of Onondaga Lake. Fast diagenesis takes place in the upper 4 cm of sediment as labile P in freshly deposited sediment is rapidly transformed due to increased microbial activity in upper oxygenated sediment layer. This more rapid P decay close to the SWI occurs simultaneously with the slower transformation of P which continues throughout the core sediments. Thus, slow diagenesis ultimately controls the long term P flux and is the focus of the Lough Neagh models.

Diagenetic model outputs in Figure 8 illustrate changes in sediment labile P as a function of time and depth for all collected Lough Neagh cores. The Foundation Model functioned well, with obtained diagenetic rates in agreement and within the range expected from eutrophic lake sediments. However, the model did not operate well at depths of 9 – 17cm in core LN15, primarily due to a substantial atypical drop in observed labile P forms.

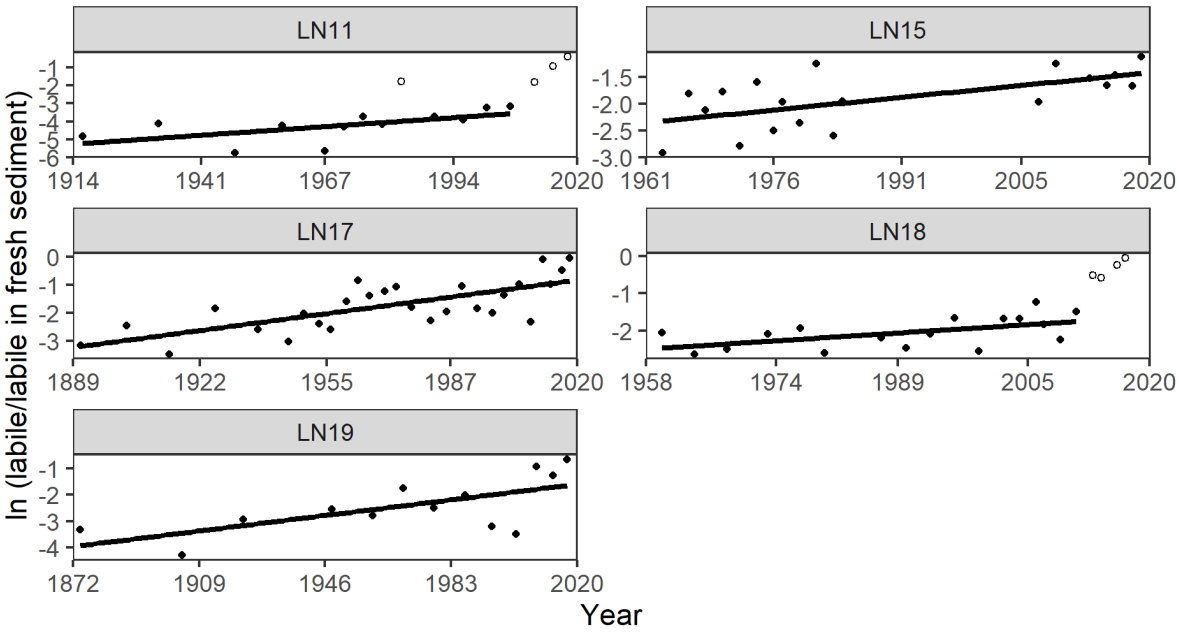

Figure 8: Diagenetic model outputs of the log-linear relationship of labile P against time for the five Lough Neagh sediment cores. Empty circles denote omitted values.

Table 1: Diagenetic rate coefficients (k_d) obtained from the regression slope in Figure 8. Coefficients are reported alongside standard error. Asterisks indicate statistical significance: p<0.5*;p<0.01**;p<0.001***.

Core ID	k_d, yr^{-1}	R^2
LN11	0.0184 (0.00730)*	0.39
LN15	0.0159 (0.00490)**	0.38
LN17	0.0184 (0.00344)***	0.53
LN18	0.0138 (0.00538)*	0.31
LN19	0.0161 (0.00545)*	0.44

The uppermost sediments of LN11 and LN18 have been omitted due to the vast contrast in labile P content at the near surface creating a distinctively different gradient from the rest of the sediment profile. In the case of LN18, approximately 50 % of TP within surface sediments (0-1 cm; 1-2 cm) consisted of NaOH-SRP. This is thought to consist primarily of Fe-P, a temporary store of volatile P, most easily recycled into the water column due to its sensitivity to changes in redox conditions. The significance of iron mediated P release has been noted in Lough Neagh (Gibson et al. 2001) due to the prevalence of oxy hydroxides at the near surface with a high affinity for P adsorption. Ferric iron becomes reduced to soluble ferrous iron in deeper anoxic sediment, whereby it diffuses upwards until re-precipitating as ferric iron, maintaining a large P binding capacity within oxygenated surface sediment (Hupfer and Lewandowski 2008).

The increased amount of P binding capacity/sites in upper sediments acts as a temporary store for P mobilised via ongoing diagenesis within both surface and deeper sediments (Boström 1988; Hupfer and Lewandowski 2008). The disproportionate concentration of Fe bound-P can control seasonal, or short-term P release, but is not significant in managing the long term retention of P (Hupfer and Lewandowski 2008).

LN11 surface sediment also had a disproportionate mass of both reactive and non-reactive NaOH extractable P (Appendix Figure 4) which tailed off quickly in comparison to other cores, although for a different reason compared to LN18. Radiometric dating identified a peak in unsupported ^{210}Pb below the sediment surface (see section 3.1), suggesting that a possible recent increase in sedimentation may be the cause of this (Appendix Figures 1 and 2). This period of increased sedimentation corresponded to a shift in sediment composition as dry weight and LOI. An additional point at 7.5 cm in LN11 was also removed due to rapid net sedimentation at this depth.

Battarbee (1978) found considerable inter-site temporal and spatial variability from a series of cores collected from Antrim Bay (site of LN11) and Battery Bay (site of LN18). This was despite the cores being collected within a relatively close vicinity at each site, at similar depths and distance from shore. The author noted that although mean site accumulation across the profundal zone was relatively uniform, the stratigraphic record of individual cores, as highlighted by diatom biostratigraphy, reflected an alternation between fast and slow sedimentation over time within each site. These features were likely to have been formed by the sporadic redistribution of surficial sediment. The abrupt change in composition at the surface of LN11 could then be the product of this intermittent redistribution of surface sediments. Antrim Bay is situated at the north-east corner of the Lough, at the downward end of the prevailing south-west winds, which may cause the sediments hereto be more frequently exposed to turbulent conditions. This would give rise to higher rates of resuspension and the removal of unconsolidated sediment. It may also increase the possibility of larger mass movement of sediment due to storm events.

Otherwise, the observed difference in gradients in LN11 and LN18 could indicate the presence of faster recycling of P-material at near surface, as previously recognised in the surface sediments of Lake Onondaga (Penn et al. 1995). If this were the case, the diagenetic

rate values (k_d) would be 0.198 and 0.115 yr^{-1} for LN11 and LN18, respectively, significantly larger than the observed slow rates in Lough Neagh. Penn et al. (1995) suggested that fast diagenesis can vary substantially throughout the year and be heavily influenced by discrete deposition events. Thus, the fast rate is not representative of the long term P flux which ultimately governs lake recovery. Instead, it would be the background slow labile P decay rate that coincides with the fast decay that would delay lake recovery. 'Fast rates' for Lough Neagh would still be over 20 times slower than that of Onondaga (4.8 yr^{-1}), being more similar to the slow diagenetic rate in that lake of 0.11 yr^{-1}. Removing these points in LN11 and LN18 reduced distortion of the slower diagenesis rate, which ultimately controls lake recovery. The sampling of five cores in our study helped dampen the effects of these differences in individual core characteristics.

The final range in diagenesis values obtained from the five cores was 0.0138 – 0.0184 k_d, yr^{-1} (Figure 8; Table1), this produced a mean±SE diagenesis rate of 0.0165±0.00087 yr^{-1}(CV 11.7 %). Timescales to steady state can be estimated as the reciprocal of the diagenetic rate, i.e. the time taken for the labile P concentration to diminish is effectively equivalent to the mass of P/rate of P recycling. For the purposes of this study, we have calculated time to reduce the labile P inventory by 75% as an estimated recovery. Time to immobilise 75% labile P via diagenetic mineralisation is calculated as:

$$k_d \cdot \tau_{75} = ln\left(\frac{P_{L0}}{0.25 \cdot P_{L0}}\right) = ln(4) = 1.386$$

$$\tau_{75} = 1.386/k_d \qquad (5)$$

For illustration, 90 and 50% recovery timescales would be calculated as:

$\tau_{90} = 2.303/k_d$ and $\tau_{50} = 0.693/k_d$

Utilising equation 5 above (the Foundation Model based on Penn et al. (1995)) produced an estimated timescale to 75 % recovery based on the mean diagenesis rate as follows:

$$\tau_{75} = \frac{1.386}{0.0165 \pm 0.00087} = 84 \pm 4\ years$$

This timescale derived from the mean diagenesis rate (k_d) was calculated by averaging the diagenetic rate constants in Table 1. Here we take $\tau 75$ as the standard time required for the internal P load to reduce to an insignificant amount and reach equilibrium with reduced inputs.

The timescale of approximately 84 years was based solely on P removal via mineralisation and subsequent recycling back to the water column. However, from Figure 7 it can be seen that not all of Labile A in Lough Neagh is mineralised. Instead, a measureable portion of Labile A, in addition to other potentially labile P forms included in Fraction A, persists below the active layer. Lewis et al. (2007) suggested the use of sediment burial velocity alongside P diagenesis to account for other processes which contribute to the immobilisation of P.

3.5.2 Purging factor 2 – Burial from active layer/rate of burial.

Besides losses from mineralisation, P can be sequestered and retained within lake sediments via burial by net sediment flux to the lake bed. Burial appears to be an important factor for P immobilization as chemical extractions performed on the five Lough Neagh cores have shown that a considerable amount of P remains in the sediment following the cessation of diagenesis.

HCl-P and Residual-P are expected to remain in the sediment as inert mineral and organic material. NaOH-SRP and NaOH-NRP, on the other hand, are considered bioavailable and would be expected to diminish with time. The immobilisation pathway for the NaOH extractable P forms depends on lake-specific environmental conditions and the P binding capacity within anoxic sediments beneath the active layer (Hupfer and Lewandoski 2008).

Mineralisation of biogenic-P (NaOH-NRP) occurs rapidly following deposition and continues with depth, though primarily within the active layer. Much of the solubilised P following mineralisation becomes adsorbed to iron oxyhydroxides, or assimilated into microorganisms as labile polyphosphates (Reitzel et al. 2007) before being released. These P stores are often sensitive to the reducing conditions of the deeper anoxic sediments, becoming resolubilised and diffusing upwards to be recycled in the active layer (Hupfer and Lewandoski 2008). More recalcitrant NaOH-NRP extractable P species can be formed within the sediment; a product of digenetic transformation and degradation of complex organic matter. These forms are become more likely to be removed from the P cycle preserved in the anoxic layer e.g. monoester-P (half-life 20 - 30 years) and humic-P compounds (half-life > 80 years) (Ahlgren et al. 2005; Reitzel et al. 2007).

Another mechanism for the permanent sequestration of P is the formation of stable iron phosphate minerals, such as vivianite. Vivanite commonly forms in sediment with a high

iron to sulphur ratio such as that of Lough Neagh. Although stable in sediments, the mineral is soluble in NaOH and may explain the persistence of the typically reductive sensitive NaOH-SRP fraction deep within the sediment profile (Rothe et al. 2015).

The inclusion of burial in the condensed timescale model suggested by Lewis et al. (2007) was effective at reproducing the response times achieved from the full diagenetic model that the authors presented. Within this model, immobilisation of P through burial is described by a second purging factor as a function of the active layer depth and sediment burial velocity (ω, cm yr^{-1}).

3.5.2.1. Active layer depth

Already mentioned above, the active layer is the area in the sediment profile from the SWI to the depth where the majority of P transformation ceases, and below which P concentration becomes reasonably constant with depth. This point was more clearly defined in some cores than others. The active layer varied substantially between sites (CV 49.1%), LN15, LN17, and LN18, had similar active layer depths of 29 cm, 21 cm, and 23 cm. LN11 and LN19 exhibited comparitively shallower active layers at 8 cm and 10 cm.

3.5.2.2 Sediment burial velocity

Burial velocity was obtained from the radiometric dating and was equivalent to the time averaged sediment accumulation from the sediment water interface to the base of the active layer. Burial velocity ranged from 0.145 – 0.519 cm yr^{-1}, mean ± SE 0.315 ± 0.143 cm yr^{-1} (CV 45.5%). LN11 and LN19 were different from the other cores due to a lower sedimentation rate.

3.5.2.3 Rate of P immobilisation through burial

The rate of P removal from the active layer via downwards burial (k_b) from the active layer as calculated from equation 6 is summarised alongside the Full Model results in Table 2.

$$k_{\mathrm{b}} = \frac{\omega}{Z_{\mathrm{active}}} \quad (6)$$

k_b is the coefficient for rate of burial, i.e. the rate of labile P removal from the active layer via downwards transport from the SWI by net sediment flux to the lakebed. Burial velocity (ω) is equivalent to the mean sedimentation rate obtained from the radiometric dating. Z_{active} is the depth of the active layer defined as the layer where the majority of diagenesis occurs.

Despite large varibility in both active layer depth and burial velocity, the rate of P loss though burial for LN15, LN17, LN18 and LN19 wasrelatively constant, ranging from 0.0145 – 0.0179 yr^{-1}, mean±SE 0.0158±0.00083 yr^{-1} (CV 10.4%). LN11 was the exception to the trend at 0.0286 yr^{-1} and changing the overall mean ± SE for all five cores to 0.00184±0.00263 yr^{-1} (CV 32.0%).

3.6 Timescales to recovery using both purging factors – the Full Model

The additional effect of burial on P, alongside diagenesis (which was used in the Foundation Model), can be represented by the below (equation 7) as presented in Lewis et al. (2007).

$$\lambda = \frac{\omega}{Z_{\text{active}}} + k_{\text{d}} \quad (7)$$

k_d is the diagenetic rate coefficient from Figure 8 and burial velocity (ω) is equivalent to the mean sedimentation rate obtained from the radiometric dating. Z_{active} is the depth of the active layer defined as the layer where the majority of diagenesis occurs. λ describes the rate at which labile P is removed from the active layer through the combined diagenesis and burial processes. Timescale of 75 % recovery based on the Full Model that includes both diagenesis and burial is as follows:

Full Model:

$$\boldsymbol{\tau_{75} = \frac{1.386}{0.0349 \pm 0.00277} = 40 \pm 3\ year}$$

The mean timescale to recovery based on the Full Model is 40 ± 3 years[1]. Model inputs and outputs are summarised in Table 2. Presented as final timescales are τ50, τ75, and τ90, as the time required to immobilise 50, 75, and 90 % respectively of the labile P content in sediment

[1]The timescale derived from the application of equation (6) utilises the mean rate of P loss (λ) of the five Lough Neagh cores. This is in good agreement with the timescale obtained by individually calculating τ75 for each core and averaging the results; mean ± $SE_{\tau 75}$ 41 ± 3 years (CV 15.6 %).

active layers. Here we take τ75 as the standard time required for the internal P load to reduce to an insignificant amount and reach equilibrium with reduced inputs.

The combined rate of P loss (λ) (equation 7) ranged from 0.0302 – 0.0470 yr^{-1} mean±SE 0.0349 ± 0.0031 yr^{-1} (CV 19.9%). Burial was a significant factor accounting for 51.9%±0.03% (CV 12.5%) of the total labile P losses from active layer sediments.

Table 2: Summary of sediment model inputs including, burial velocity (ω), active layer depth (Z_{active}), diagenetic rate constant (k_d±SE), labile P loss rate constant (λ), and final model outputs with response times for Lough Neagh sediment cores in years (t_x).

Core ID	ω, cm yr^{-1}	Z_{active}, cm	k_d, yr^{-1}	ω/Z_{active}, yr^{-1}	λ, yr^{-1}	t_{50}, yr	t_{75}, yr	t_{90}, yr
LN11	0.229	8	0.0184 (0.00730)	0.0286	0.0470	15	30	49
LN15	0.519	29	0.0159 (0.00490)	0.0179	0.0338	21	41	68
LN17	0.304	21	0.0184 (0.00344)	0.0145	0.0329	21	42	70
LN18	0.377	23	0.0138 (0.00538)	0.0164	0.0302	23	46	76
LN19	0.145	10	0.0161 (0.00545)	0.0145	0.0306	23	45	75

LN11 was noticeably different from the other cores with λ, yr^{-1} between 28 – 36% higher than the other four cores analysed. Despite this, when excluding LN11, there did not appear

to be a significant effect on the final recovery estimate (τ75) other than increasing precision amongst/across the remaining estimates mean±SE of 43.6 ± 1.2 years (CV 5.6%).

The trajectory of recovery following a reduction in external loading differs from lake-to-lake, largely dependent on basin morphology and the extent and duration in loading history (Jeppesen et al. 2005). Smaller lakes with a higher rate of flushing often recover faster (in the scale of 10 years (or so)) whilst lakes with a longer retention time, such as Lough Neagh (1.3 years), exhibit symptoms of eutrophication that can endure for decades.

4.0 Conclusion and Recommendations

The release of phosphorus from Lough Neagh sediments has been observed since the 1960s, however since the mid 1990's a change in magnitude has occurred in the mass of P released (McElarney et al. 2021). A larger mass of P is released each summer in recent years and this has the ability to impact the effectiveness of management measures in the Lough Neagh catchment. Phosphorus release from the sediment has increased in the summer due to changes in lake conditions, especially water temperature and nitrate concentration. These factors can enhance release of P stored in lake sediment.

This research project has quantified and characterised the sediment P in Lough Neagh and produced "timescales to recovery" models. These models estimate how long it will take for the P stored in sediment to be flushed from the lake.

We used the P chemistry and dating information from sediment cores to derive an estimate of the time that it will take for the stored sediment P to be naturally removed from the lake. A model that included two major purging factors was successfully developed and provided a timescale of approximately 40 years.

This estimate of water quality recovery time (from internally loaded P) will allow lake managers to take internally release P into account in setting their water quality targets. It is important to note that the estimated timeframes provided by the models do not take into account continued catchment inputs to the lake, which must be continued to be managed responsibly.

Recommendations arising as a result of the project work include advice to produce lake specific timescales of recovery models for Northern Irish lakes that show evidence of internal loading.

We also recommend further investigation of the relative magnitudes of internal and external load for these lakes, including Lough Neagh. This may be desk based and involve the use of process based models. This will help estimate how much internal loading is adding to the current TP concentrations in the lakes.

Reference list

AHLGREN, J., TRANVIK, L., GOGOLL, A., WALDEBÄCK, M., MARKIDES, K. & RYDIN, E. 2005. Sediment depth attenuation of biogenic phosphorus compounds measured by 31P NMR. Environmental Science & Technology, 39, 867-872.

ANDERSEN, J. M. 1976. An ignition method for determination of total phosphorus in lake sediments. Water research, 10, 329-331.

APPLEBY, P. 2001. Chronostratigraphic techniques in recent sediments. Tracking environmental change using lake sediments. Springer.

APPLEBY, P., NOLAN, P., GIFFORD, D., GODFREY, M., OLDFIELD, F., ANDERSON, N. & BATTARBEE, R. 1986. 210 Pb dating by low background gamma counting. Hydrobiologia, 143, 21-27.

APPLEBY, P. & OLDFIELD, F. 1992. Applications of lead-210 to sedimentation studies. Uranium-series disequilibrium: applications to earth, marine, and environmental sciences. 2. ed.

APPLEBY, P. G. & OLDFIELD, F. 1978. The calculation of lead-210 dates assuming a constant rate of supply of unsupported 210Pb to the sediment. Catena, 5, 1-8.

BACHMANN, R. W., HOYER, M. V. & CANFIELD, D. E. 2018. Possible sediment mixing and the disparity between field measurements and paleolimnological inferences in shallow Iowa Lakes in the Midwestern United States. Geosciences, 8, 40.

BATTARBEE, R. W. 1978. Observations on the recent history of Lough Neagh and its drainage basin. Philosophical Transactions of the Royal Society of London. B, Biological Sciences, 281, 303-345.

BIRK, S., CHAPMAN, D., CARVALHO, L., SPEARS, B. M., ANDERSEN, H. E., ARGILLIER, C., AUER, S., BAATTRUP-PEDERSEN, A., BANIN, L. & BEKLIOĞLU, M. 2020. Impacts of multiple stressors on freshwater biota across spatial scales and ecosystems. Nature Ecology & Evolution, 4, 1060-1068.

BOSTRÖM, B., ANDERSEN, J. M., FLEISCHER, S. & JANSSON, M. 1988. Exchange of phosphorus across the sediment-water interface. Phosphorus in freshwater ecosystems. Springer.

CARTER, C. & MURPHY, P. 1993. The macroinvertebrate fauna of Lough Neagh. Lough Neagh. Springer.

CHAPRA, S. C. 2008. Surface water-quality modeling, Waveland press.

DEAN, W. E. 1974. Determination of carbonate and organic matter in calcareous sediments and sedimentary rocks by loss on ignition; comparison with other methods. Journal of Sedimentary Research, 44, 242-248.

DOUGLAS, R. W. & RIPPEY, B. 2000. The random redistribution of sediment by wind in a lake. Limnology and Oceanography, 45, 686-694.

EISENREICH, S., BANNERMAN, R. & ARMSTRONG, D. 1975. A simplified phosphorus analysis technique. Environmental letters, 9, 43-53.

EUROPEAN ENVIRONMENT AGENCY 2018. European waters assessment of status and pressures 2018. EEA Report.

EUROPEAN COMMISSION 1992. Council Directive 92/43/EEC of 21 May 1992 on the conservation of natural habitats and of wild fauna and flora.

EUROPEAN COMMISSION 2000. Council Directive 2000/60/EC of the European Parliament and of the Council of 23.10.2000 establishing a framework for Community action in the field of water policy. European Union, Brussels.

EUROPEAN COMMISSION 2009. Directive 2009/147/EC of the European Parliament and of the Council of 30 November 2009 on the conservation of wild birds.

FLETCHER, C. L. 1990. The recent sedimentary history and contemporary budges of zinc, copper and lead in Lough Neagh, Northern Ireland. Unpublished DPhil thesis of the University of Ulster

FOY, R., LENNOX, S. & GIBSON, C. 2003. Changing perspectives on the importance of urban phosphorus inputs as the cause of nutrient enrichment in Lough Neagh. Science of the Total Environment, 310, 87-99.

FOY, R., SMITH, R., JORDAN, C. & LENNOX, S. 1995. Upward trend in soluble phosphorus loadings to Lough Neagh despite phosphorus reduction at sewage treatment works. Water Research, 29, 1051-1063.

FURUMAI, H. & OHGAKI, S. 1982. Fractional composition of phosphorus forms in sediments related to release. Water Science and Technology, 14, 215-226.

GIBSON, C. E., WANG, G., FOY, R. H. & LENNOX, S. D. 2001. The importance of catchment and lake processes in the phosphorus budget of a large lake. Chemosphere, 42, 215-220.

HIELTJES, A. H. & LIJKLEMA, L. 1980. Fractionation of inorganic phosphates in calcareous sediments. Journal of Environmental Quality, 9, 405-407.

HILTON, J., LISHMAN, J. & MILLINGTON, A. 1986. A comparison of some rapid techniques for the measurement of density in soft sediments. Sedimentology, 33, 777-781.

HUPFER, M. & LEWANDOWSKI, J. 2008. Oxygen controls the phosphorus release from lake sediments–a long-lasting paradigm in limnology. International Review of Hydrobiology, 93, 415-432.

IUCN 2020. Anguilla anguilla. The IUCN Red List of Threatened Species 2020: e.T60344A152845178.

JENSEN, H. S. & ANDERSEN, F. O. 1992. Importance of temperature, nitrate, and pH for phosphate release from aerobic sediments of four shallow, eutrophic lakes. Limnology and Oceanography, 37, 577-589.

JEPPESEN, E., PEDER JENSEN, J., SØNDERGAARD, M., LAURIDSEN, T. & LANDKILDEHUS, F. 2000. Trophic structure, species richness and biodiversity in Danish lakes: changes along a phosphorus gradient. Freshwater biology, 45, 201-218.

JEPPESEN, E., SØNDERGAARD, M., JENSEN, J. P., HAVENS, K. E., ANNEVILLE, O., CARVALHO, L., COVENEY, M. F., DENEKE, R., DOKULIL, M. T. & FOY, B. 2005. Lake responses to reduced nutrient loading–an analysis of contemporary long-term data from 35 case studies. Freshwater Biology, 50, 1747-1771.

LEWIS, G. N., AUER, M. T., XIANG, X. & PENN, M. R. 2007. Modeling phosphorus flux in the sediments of Onondaga Lake: Insights on the timing of lake response and recovery. Ecological Modelling, 209, 121-135.

LUKKARI, K., HARTIKAINEN, H. & LEIVUORI, M. 2007a. Fractionation of sediment phosphorus revisited. I: Fractionation steps and their biogeochemical basis. Limnology and Oceanography: Methods, 5, 433-444.

LUKKARI, K., LEIVUORI, M. & HARTIKAINEN, H. 2007b. Fractionation of sediment phosphorus revisited: II. Changes in phosphorus fractions during sampling and storing in the presence or absence of oxygen. Limnology and Oceanography: Methods, 5, 445-456.

MACKERETH, F. 1969. A short core sampler for subaqueous deposits. Limnology and Oceanography, 14, 145-151.

MAY, L., DEFEW, L., BENNION, H. & KIRIKA, A. 2012. Historical changes (1905–2005) in external phosphorus loads to Loch Leven, Scotland, UK. Loch Leven: 40 years of scientific research. Springer.

MCELARNEY, Y., RIPPEY, B., MILLER, C., ALLEN, M. AND UNWIN, A. 2021. The long-term response of lake nutrient and chlorophyll concentrations to changes in nutrient loading in Ireland's largest lake, Lough Neagh. Biology and Environment. In press.

MURPHY, J. & RILEY, J. P. 1962. A modified single solution method for the determination of phosphate in natural waters. Analytica chimica acta, 27, 31-36.

NI WATER. 2012. Northern Ireland Water Limited Water Resources Management Plan 2012

NÜRNBERG, G. K. 2009. Assessing internal phosphorus load–problems to be solved. Lake and Reservoir Management, 25, 419-432.

OECD 1982. Eutrophication of waters: monitoring, assessment and control, Unversity of Michigan.

OSTROFSKY, M. L. 2012. Differential post-depositional mobility of phosphorus species in lake sediments. Journal of paleolimnology, 48, 559-569.

PENN, M. R., AUER, T., VAN ORMAN, E. L. & KORIENEK, J. J. 1995. Phosphorus diagenesis in lake sediments: investigations using fractionation techniques. Marine and Freshwater Research, 46, 89-99.

REITZEL, K., AHLGREN, J., DEBRABANDERE, H., WALDEBÄCK, M., GOGOLL, A., TRANVIK, L. & RYDIN, E. 2007. Degradation rates of organic phosphorus in lake sediment. Biogeochemistry, 82, 15-28.

RIPPEY, B. 1980. The release of silicon and phosphorus from the sediments of Lough Neagh. Unpublished DPhil thesis of the New University of Ulster.

ROTHE, M., KLEEBERG, A., GRÜNEBERG, B., FRIESE, K., PÉREZ-MAYO, M. & HUPFER, M. 2015. Sedimentary sulphur: iron ratio indicates vivianite occurrence: a study from two contrasting freshwater systems. Plos one, 10, e0143737.

ROWAN, D., CORNETT, R., KING, K. & RISTO, B. 1995. Sediment focusing and 210 Pb dating: a new approach. Journal of Paleolimnology, 13, 107-118.

RYDIN, E. 2000. Potentially mobile phosphorus in Lake Erken sediment. Water Research, 34, 2037-2042.

SCHINDLER, D. W. 1977. Evolution of phosphorus limitation in lakes. Science, 195, 260-262.

SCHINDLER, D. W. 2006. Recent advances in the understanding and management of eutrophication. Limnology and oceanography, 51, 356-363.

SMITH, V. H. & SCHINDLER, D. W. 2009. Eutrophication science: where do we go from here? Trends in ecology & evolution, 24, 201-207.

SØNDERGAARD, M., BJERRING, R. & JEPPESEN, E. 2013. Persistent internal phosphorus loading during summer in shallow eutrophic lakes. Hydrobiologia, 710, 95-107.

SØNDERGAARD, M., JENSEN, J. P. & JEPPESEN, E. 2003. Role of sediment and internal loading of phosphorus in shallow lakes. Hydrobiologia, 506, 135-145.

VOLLENWEIDER, R. A. 1968. Scientific fundamentals of the eutrophication of lakes and flowing waters, with particular reference to nitrogen and phosphorus as factors in eutrophication, OECD Paris.

WOOD, R. & SMITH, R. 2013. Lough Neagh: the ecology of a multipurpose water resource, Springer Science & Business Media.

Appendix

- **LN11**

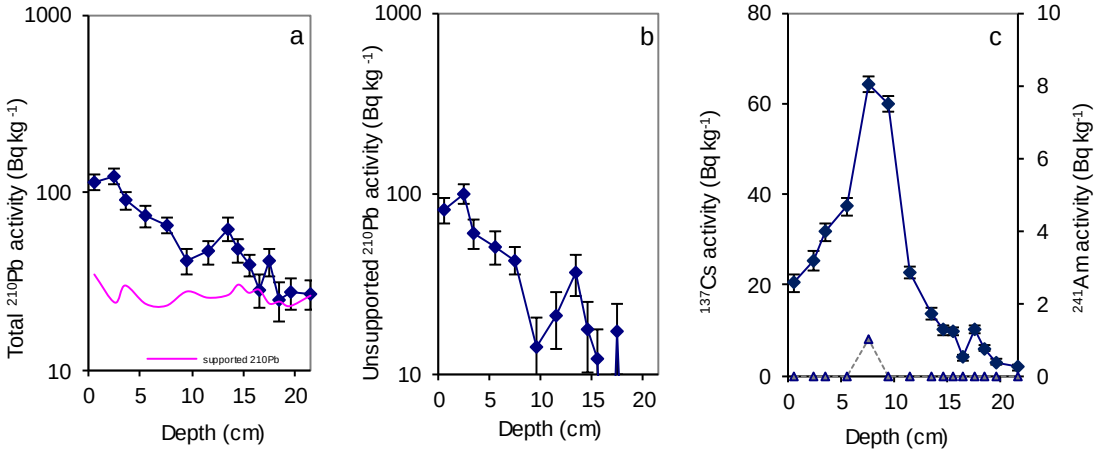

Figure 1: Fallout radionuclide concentrations in core LN11 taken from Lough Neagh, showing (a) total ^{210}Pb, (b) unsupported ^{210}Pb, and (c) ^{137}Cs and ^{241}Am concentrations versus depth.

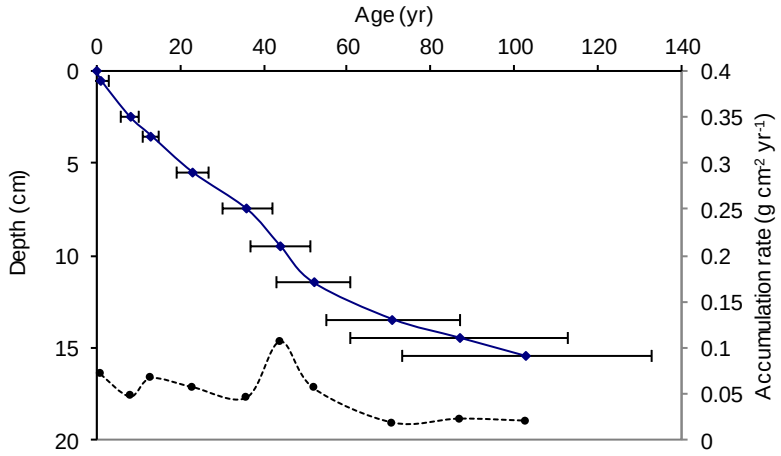

Figure 2: Radiometric chronology of core LN11 taken from Lough Neagh, showing the CRS model ^{210}Pb dates and sedimentation rates. The solid line shows age while the dashed line indicates sedimentation rate.

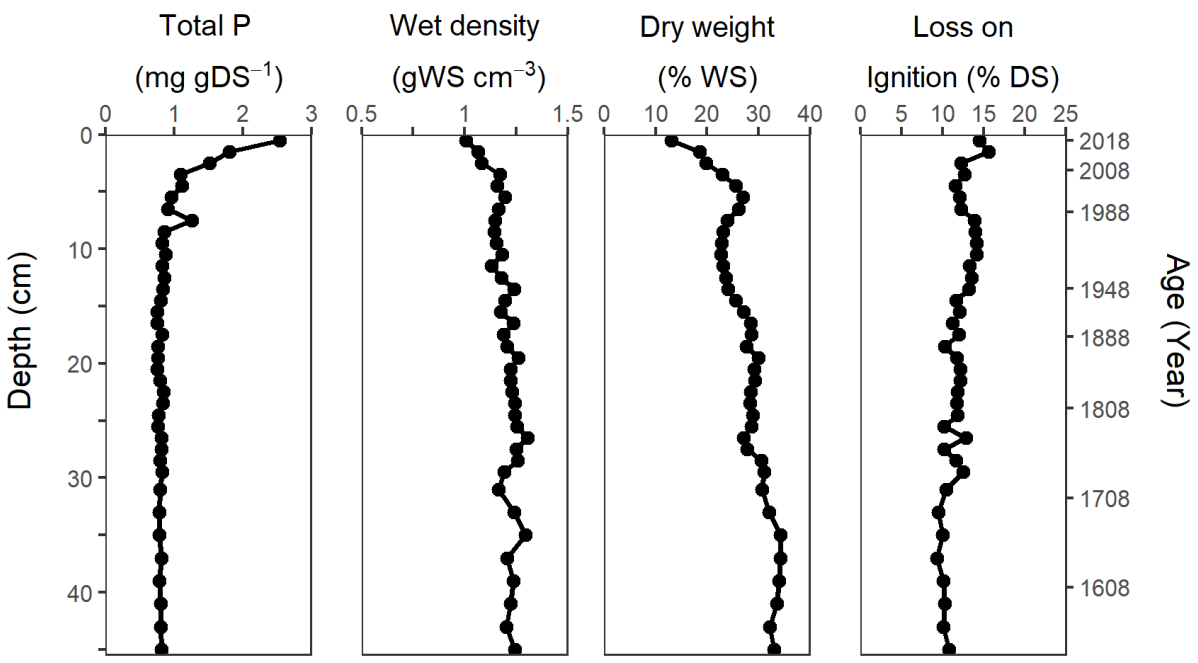

Figure 3: Basic sediment overview for core LN11 to 45 cm. Total phosphorus, wet density, dry weight as a percentage of wet weight, and loss on ignition (proxy for organic matter content) as a percentage of dry sediment weight. Sediment age on the secondary y-axis obtained from ^{210}Pb CRS model chronologies until 16 cm (1916) and extrapolated until 45 cm.

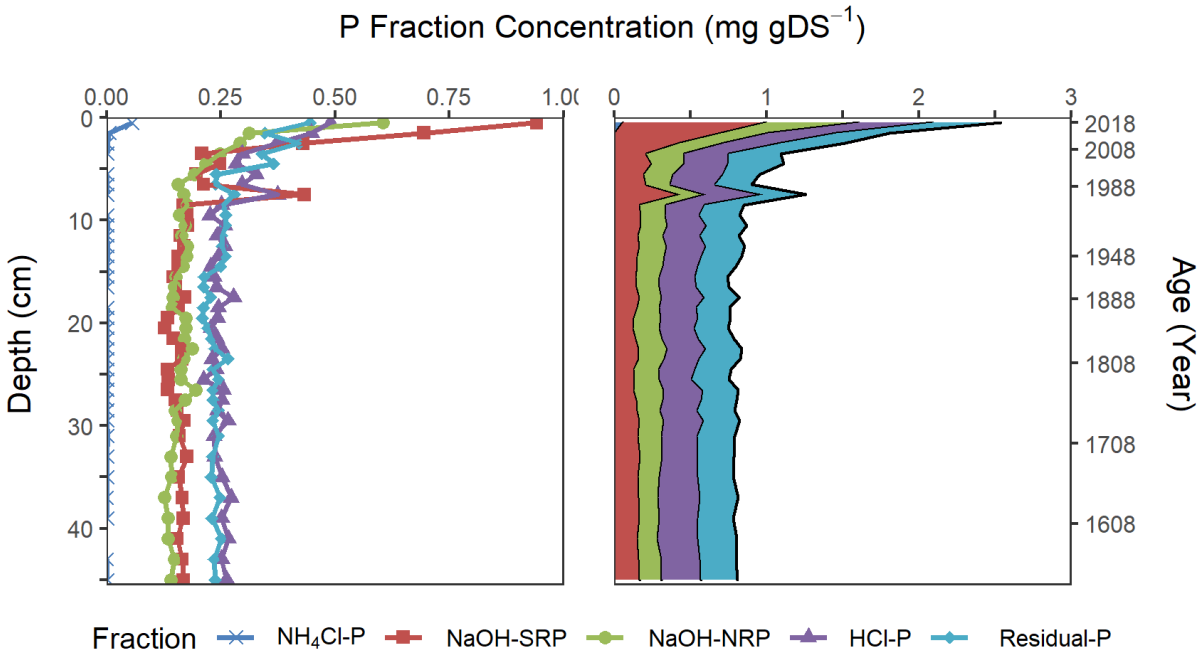

Figure 4: Vertical profiles of extracted P fractions in core LN11 in mg gDS^{-1} until 45 cm. For clearer interpretation, variations in P fraction concentration is displayed both individually (left) and stackable area (right). The sum of the 5 fractions is equivalent to total extracted P. Sediment age on the secondary y-axis obtained from ^{210}Pb CRS model chronologies until 16 cm (1916) and extrapolated until 45 cm.

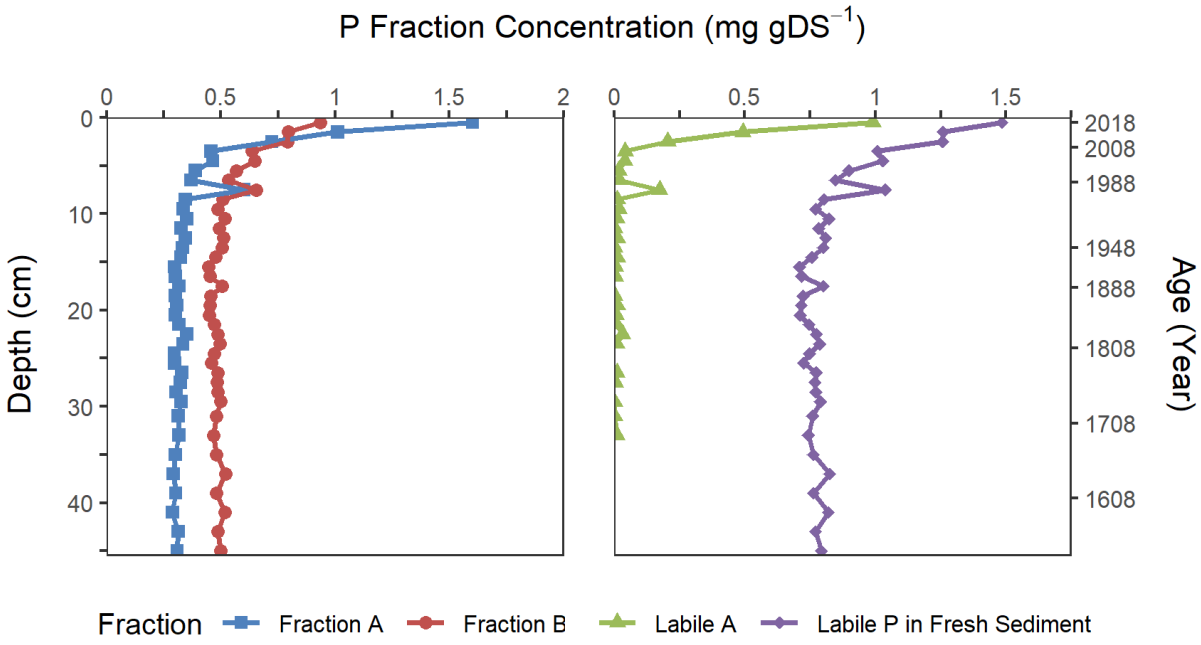

Figure 5: Left displays vertical profiles of Fraction A (sum of NH_4Cl; NaOH-SRP; NaOH-NRP) and Fraction B (sum of HCl-P; Residual-P) in core LN11 in mg gDS^{-1} until 45 cm. Right displays profile of Labile A (bioavailable-P) present in the sediment at time of analysis and Labile P at time of deposition to sediment surface. Sediment age on the secondary y-axis obtained from ^{210}Pb CRS model chronologies until 37 cm (1890) and extrapolated until 45 cm.

- **LN15**

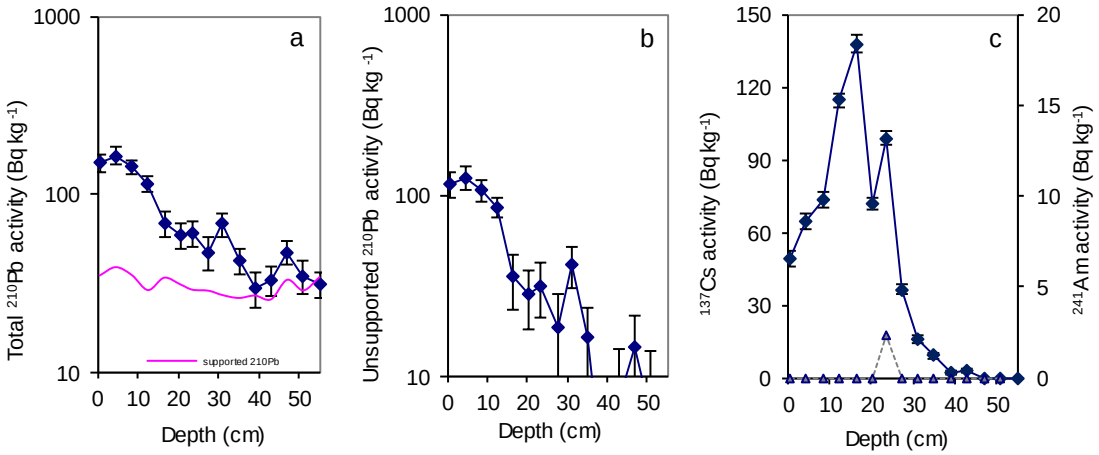

Figure 6: Fallout radionuclide concentrations in core LN15 taken from Lough Neagh, showing (a) total ^{210}Pb, (b) unsupported ^{210}Pb, and (c) ^{137}Cs and ^{241}Am concentrations versus depth.

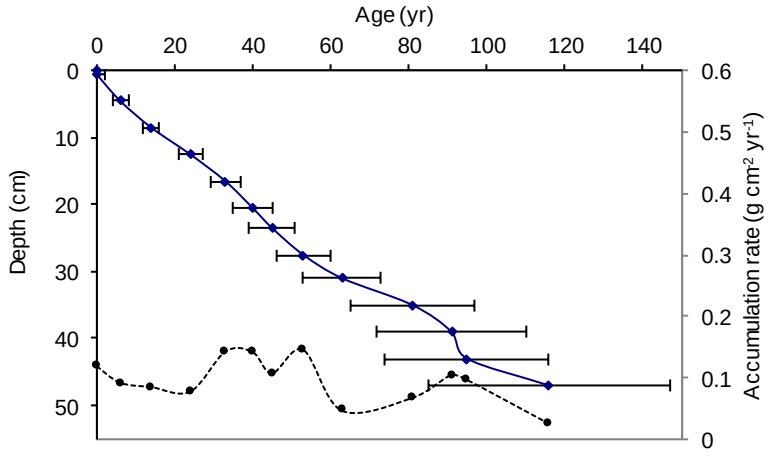

Figure 7: Radiometric chronology of core LN15 taken from Lough Neagh, showing the CRS model ^{210}Pb dates and sedimentation rates. The solid line shows age while the dashed line indicates sedimentation rate.

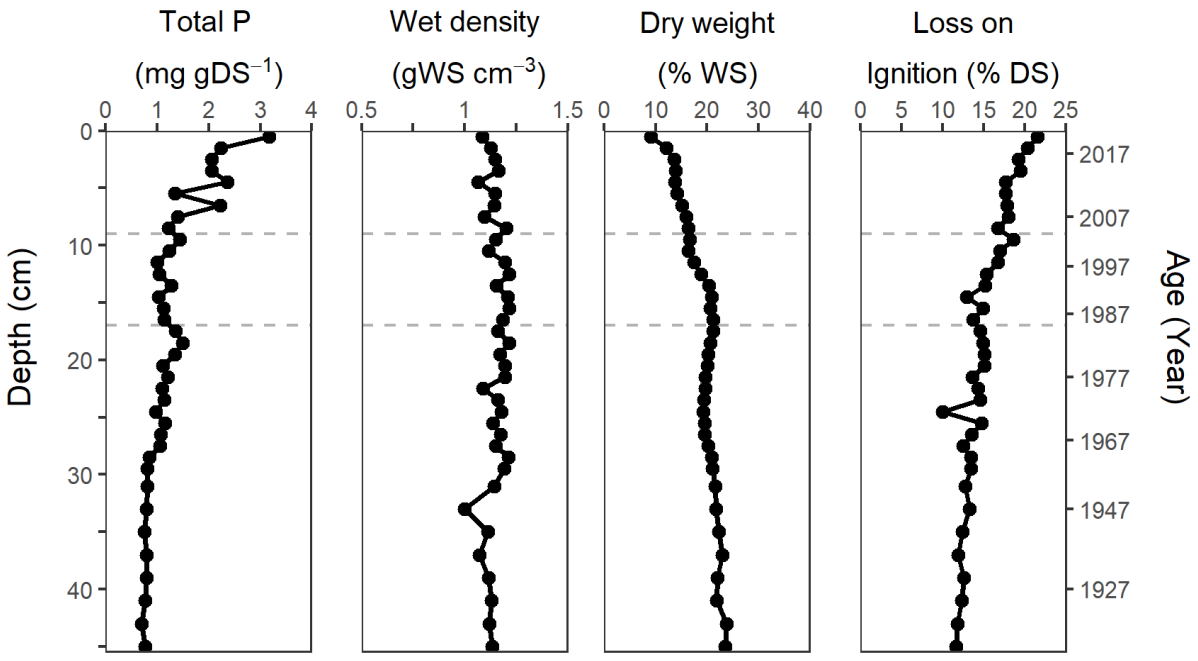

Figure 8: Basic sediment overview for core LN15 to 45 cm. Total phosphorus, wet density, dry weight as a percentage of wet weight, and loss on ignition (proxy for organic matter content) as a percentage of dry sediment weight. Sediment age on the secondary y-axis obtained from ^{210}Pb CRS model chronologies until 45 cm. Dashed lines highlight portion of the sediment profile between 9-17 cm where the diagenetic model was unable to function.

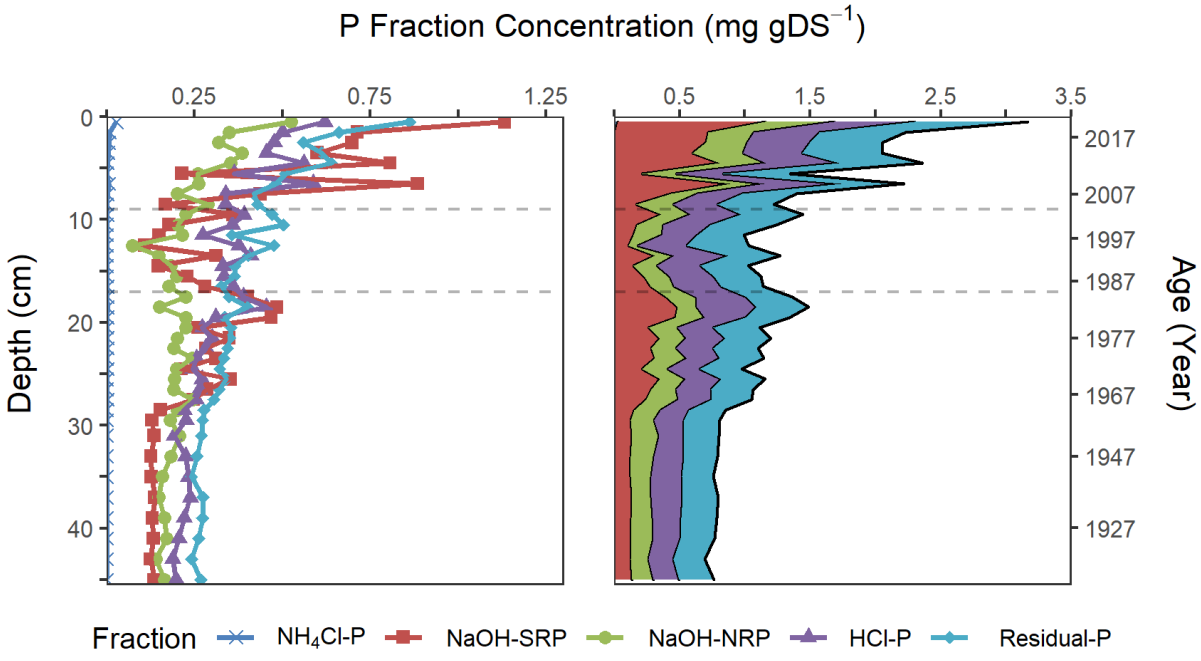

Figure 9: Vertical profiles of extracted P fractions in core LN15 in mg gDS^{-1} until 45 cm. For clearer interpretation, variations in P fraction concentration is displayed both individually (left) and stackable area (right). The sum of the 5 fractions is equivalent to total extracted P. Sediment age on the secondary y-axis obtained from ^{210}Pb CRS model chronologies until 45 cm. Dashed lines highlight portion of the sediment profile between 9-17 cm where the diagenetic model was unable to function.

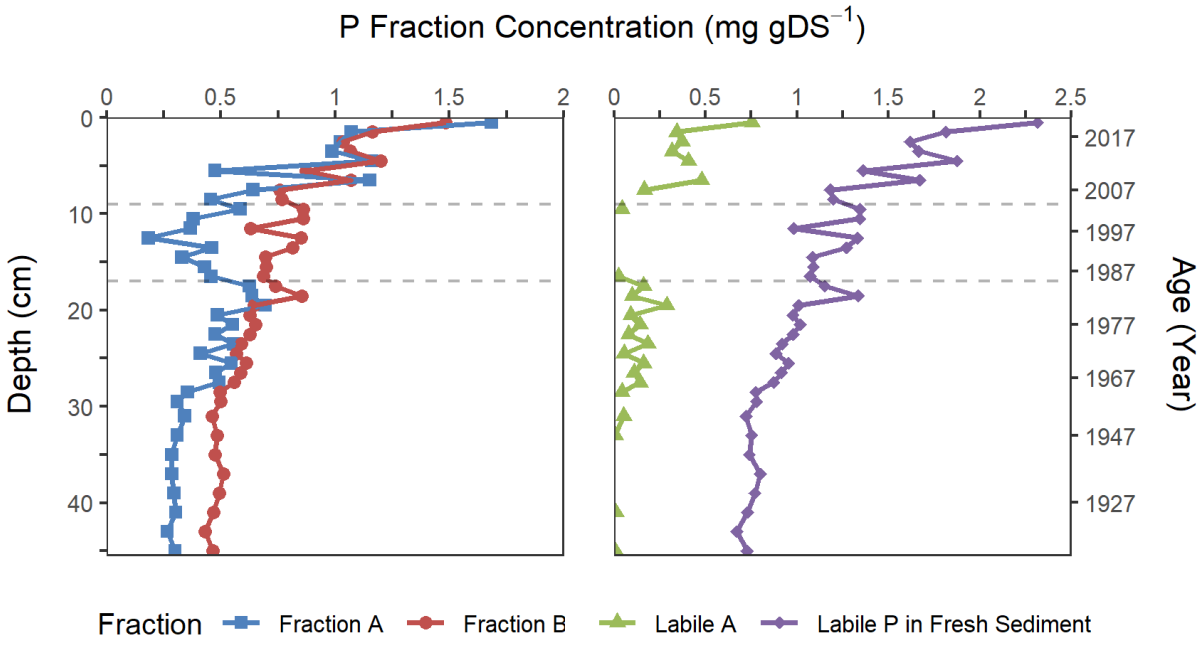

Figure 10: Left displays vertical profiles of Fraction A (sum of NH_4Cl; NaOH-SRP; NaOH-NRP) and Fraction B (sum of HCl-P; Residual-P) in core LN15 in mg gDS^{-1} until 45 cm. Right displays profile of Labile A (bioavailable-P) present in the sediment at time of analysis and Labile P at time of deposition to sediment surface. Sediment age on the secondary y-axis obtained from ^{210}Pb CRS model chronologies until 45 cm. Dashed lines highlight portion of the sediment profile between 9-17 cm where the diagenetic model was unable to function.

- **LN17**

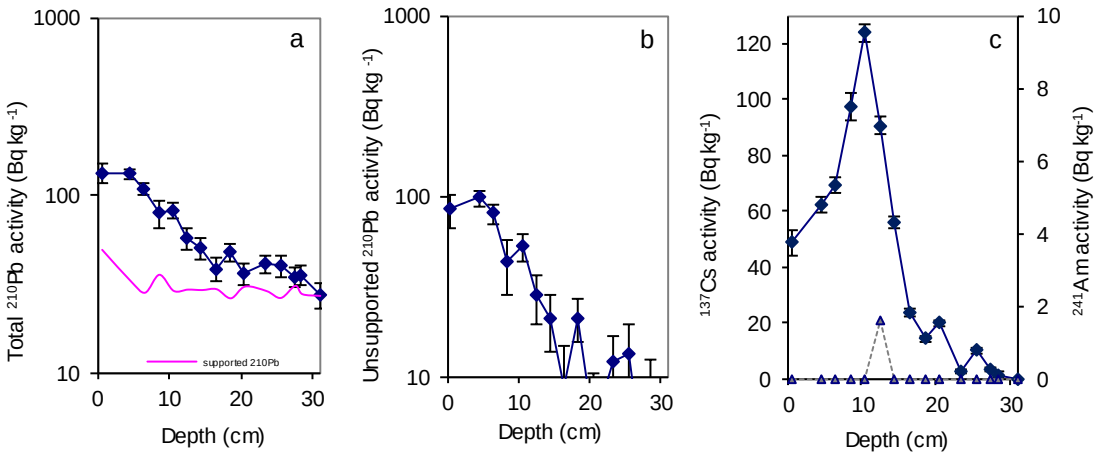

Figure 11: Fallout radionuclide concentrations in core LN17 taken from Lough Neagh, showing (a) total ^{210}Pb, (b) unsupported ^{210}Pb, and (c) ^{137}Cs and ^{241}Am concentrations versus depth.

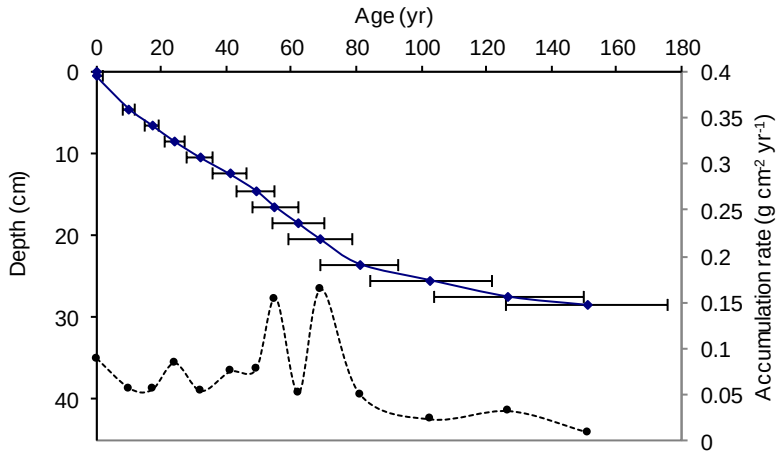

Figure 12: Radiometric chronology of core LN17 taken from Lough Neagh, showing the CRS model ^{210}Pb dates and sedimentation rates. The solid line shows age while the dashed line indicates sedimentation rate.

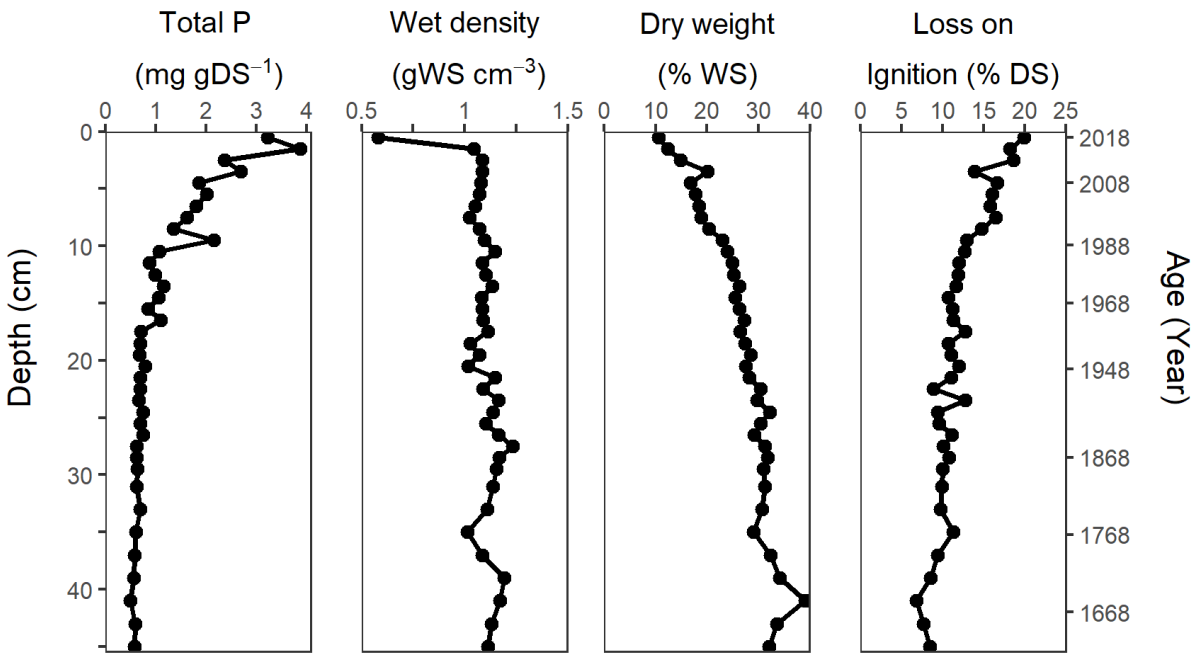

Figure 13: Basic sediment overview for core LN17 to 45 cm. Total phosphorus, wet density, dry weight as a percentage of wet weight, and loss on ignition (proxy for organic matter content) as a percentage of dry sediment weight. Sediment age on the secondary y-axis obtained from ^{210}Pb CRS model chronologies until 29 cm (1867) and extrapolated until 45 cm.

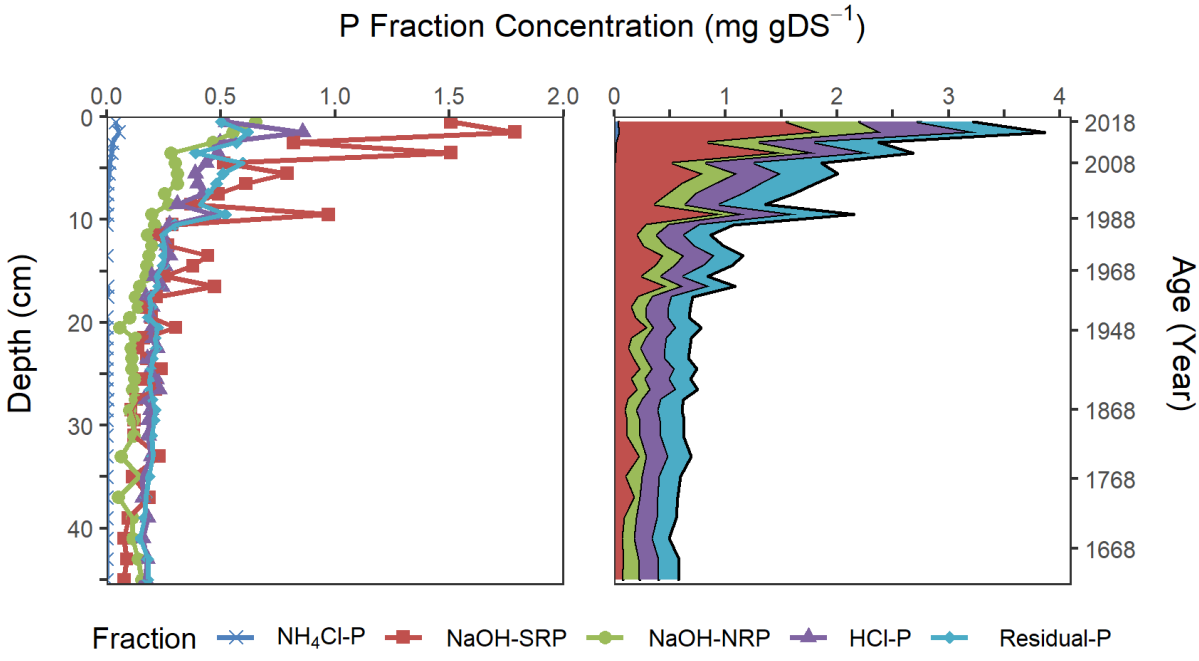

Figure 14: Vertical profiles of extracted P fractions in core LN17 in mg gDS^{-1} until 45 cm. For clearer interpretation, variations in P fraction concentration is displayed both individually (left) and stackable area (right). The sum of the 5 fractions is equivalent to total extracted P. Sediment age on the secondary y-axis obtained from ^{210}Pb CRS model chronologies until 16 cm (1916) and extrapolated until 45 cm.

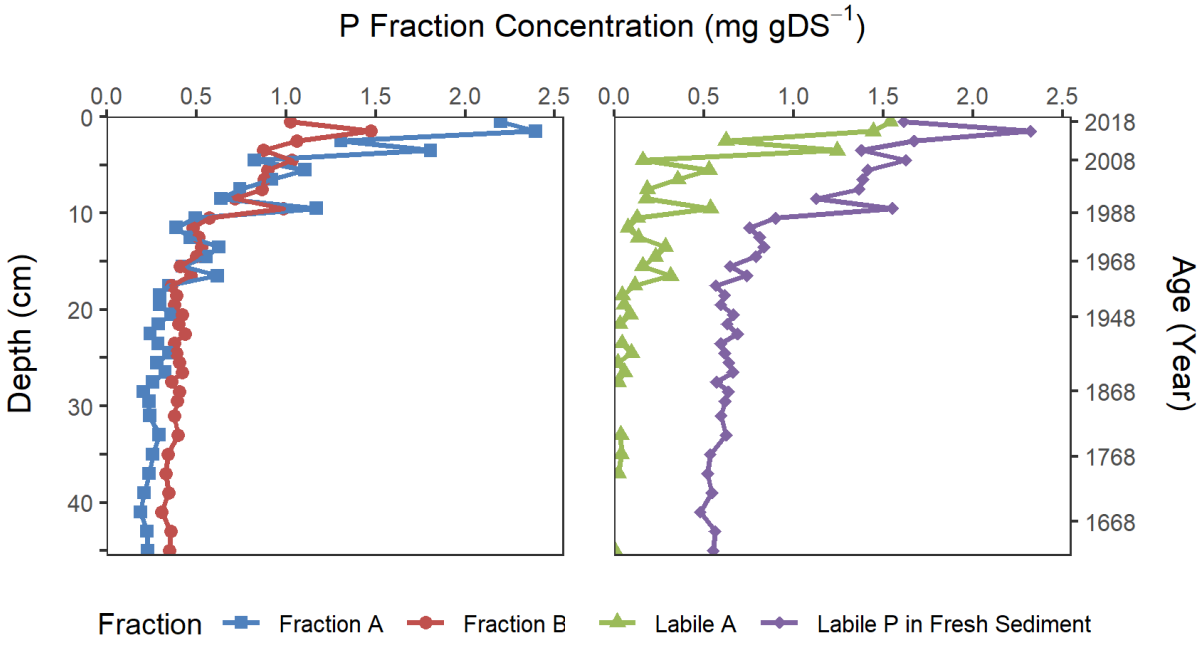

Figure 15: Left displays vertical profiles of Fraction A (sum of NH_4Cl; NaOH-SRP; NaOH-NRP) and Fraction B (sum of HCl-P; Residual-P) in core LN17 in mg gDS^{-1} until 45 cm. Right displays profile of Labile A (bioavailable-P) present in the sediment at time of analysis and Labile P at time of deposition to sediment surface. Sediment age on the secondary y-axis obtained from ^{210}Pb CRS model chronologies 29 cm (1867) and extrapolated until 45 cm.

- **LN19**

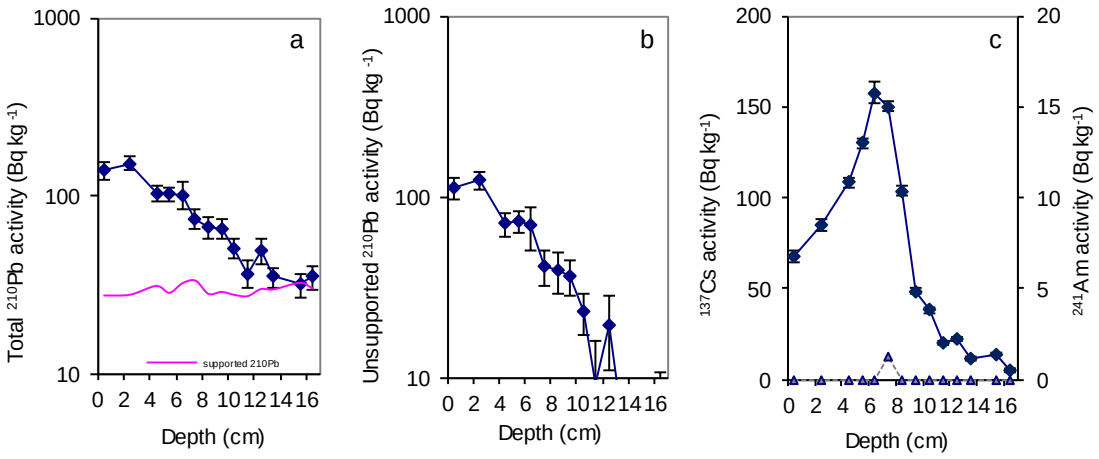

Figure 16: Fallout radionuclide concentrations in core LN19 taken from Lough Neagh, showing (a) total ^{210}Pb, (b) unsupported ^{210}Pb, and (c) ^{137}Cs and ^{241}Am concentrations versus depth.

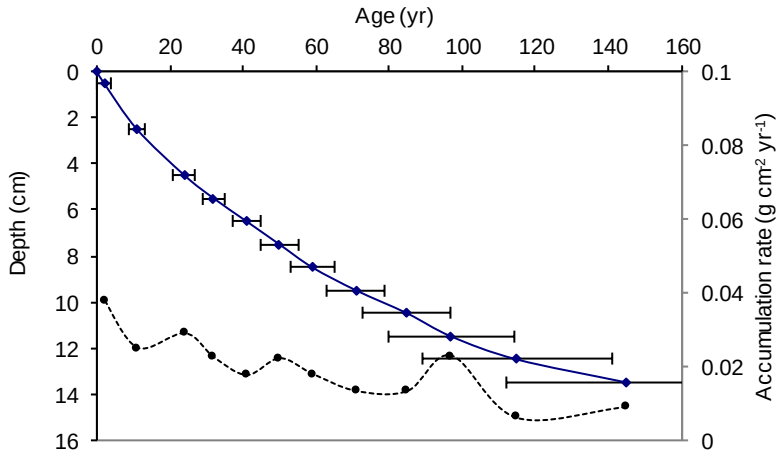

Figure 17: Radiometric chronology of core LN19 taken from Lough Neagh, showing the CRS model ^{210}Pb dates and sedimentation rates. The solid line shows age while the dashed line indicates sedimentation rate.

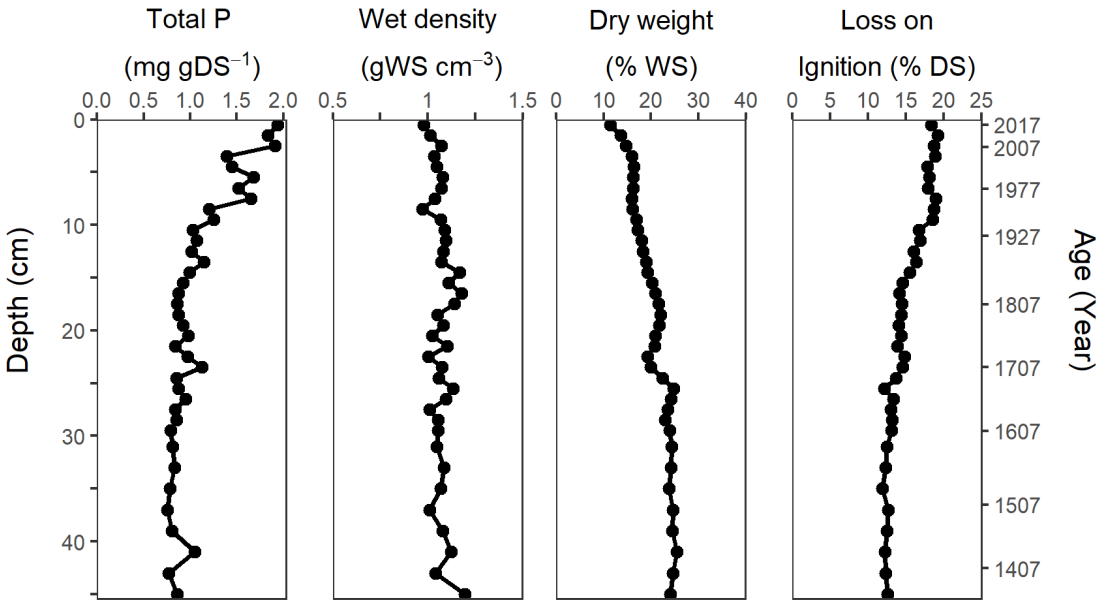

Figure 18: Basic sediment overview for core LN19 to 45 cm. Total phosphorus, wet density, dry weight as a percentage of wet weight, and loss on ignition (proxy for organic matter content) as a percentage of dry

sediment weight. Sediment age on the secondary y-axis obtained from ^{210}Pb CRS model chronologies until 14cm (1874) and extrapolated until 45 cm.

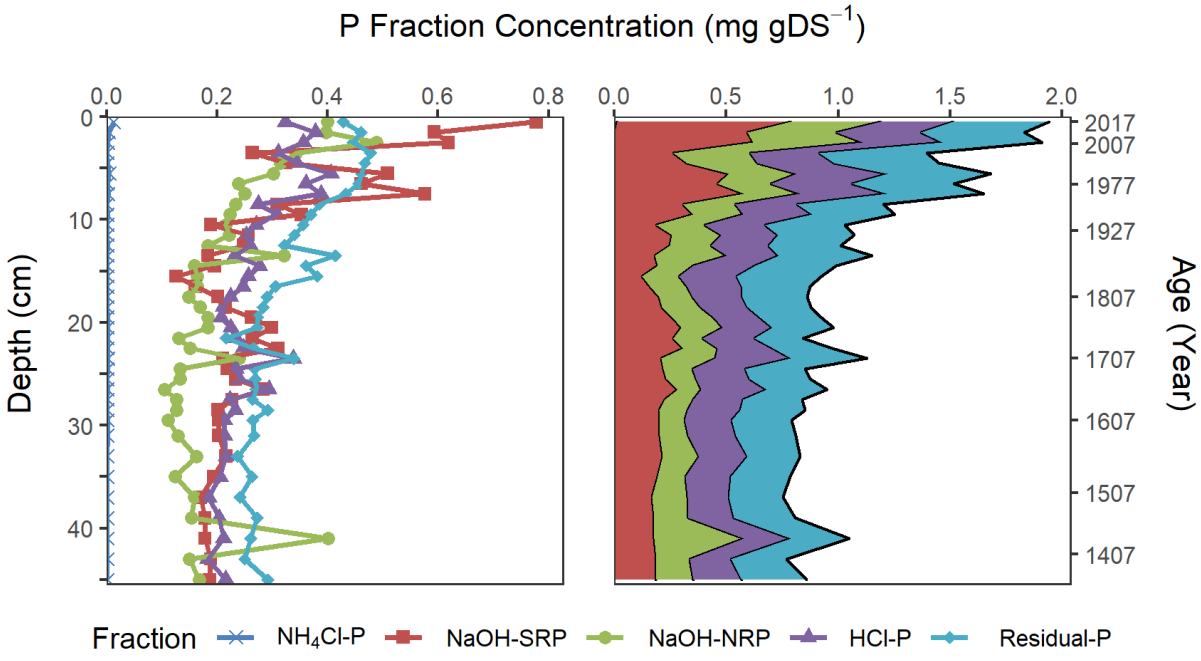

Figure 19: Vertical profiles of extracted P fractions in core LN19 in mg gDS^{-1} until 45 cm. For clearer interpretation, variations in P fraction concentration is displayed both individually (left) and stackable area (right). The sum of the 5 fractions is equivalent to total extracted P. Sediment age on the secondary y-axis obtained from ^{210}Pb CRS model chronologies until 14 cm (1874) and extrapolated until 45 cm.

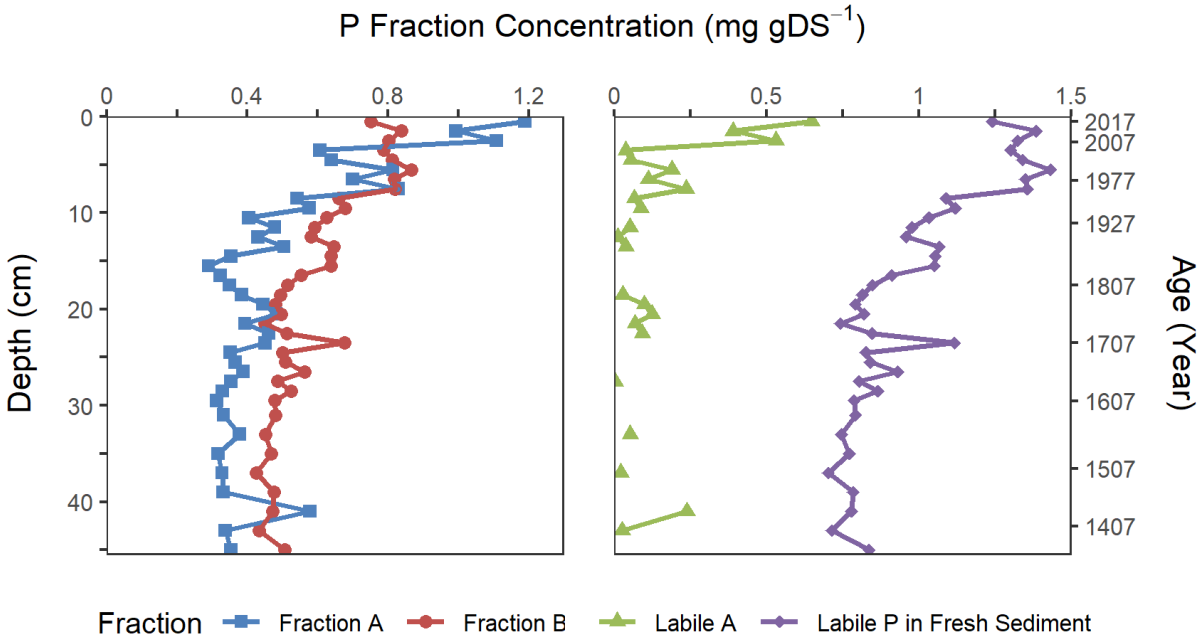

Figure 20: Left displays vertical profiles of Fraction A (sum of NH_4Cl; NaOH-SRP; NaOH-NRP) and Fraction B (sum of HCl-P; Residual-P) in core LN19 in mg gDS^{-1} until 45 cm. Right displays profile of Labile A (bioavailable-P) present in the sediment at time of analysis and Labile P at time of deposition to sediment surface. Sediment age on the secondary y-axis obtained from ^{210}Pb CRS model chronologies until 14 cm (1874) and extrapolated until 45 cm.